A Novel Membrane Separation Process Using Electron-Charge Transfer Complexes

Yin Mou
B.S. Peking University, 1989

A thesis submitted to the faculty of
the Oregon Graduate Institute of Science & Technology
in partial fulfillment of the
requirements for the degree

Master of Science
in
Chemistry

October 1994

The thesis "A novel membrane separation process using electron charge transfer complexes" by Yin Mou has been examined and approved by the following Examination Committee:

David W. Grainger, Thesis advisor
Associate Professor

V. Renganathan
Associate Professor

Paul G. Tratnyek
Assistant Professor

Acknowledgements

I am deeply indebted to Dr. David W. Grainger, my advisor, for his guidance, instruction, and understanding throughout this work. Without his patience, support and helpful suggestions, I would have not been able to complete my thesis work successfully.

I am very grateful to my committee members, Dr. V. Renganathan and Dr. Paul G. Tratnyek, for their time spent reviewing this document and providing me with many valuable comments. I would like to thank Dr. Geoffrey A. Russell and Dr. George D. Case for their support and inspirational conversations, Kevin M. Maloney for his generous assistance with English on this thesis and also countless help over the past three years. Also, I would like to express my appreciation to Vernon Booth, Andrew Stein, Guoqiang Mao, Dr. Qun Song, Xin Huang and Hua Yu for sharing instruments and lab space with me, providing me with helpful suggestions, discussions and friendship. Many thanks to all the faculty, staff and students in the Department of Chemistry, Biochemistry, and Molecular Biology, for providing such a supportive environment and wonderful companionship. Special thanks to Nancy Christie.

Table of Contents

List of Tables

List of Figures

List of Schemes

Abstract

A novel membrane separation process using electron charge transfer complexes

Yin Mou, M.S.

Supervising Professor: David W. Grainger

N-substituted maleimides have been shown to have specific complexing properties with aromatic compounds via electron donor-acceptor interactions. Complexing strengths of N-substituted maleimides towards various aromatic compounds vary with maleimide chemistry. Substitution on both maleimides and aromatic compounds changes electronic properties of these compounds, which in turn changes complexation strengths. Complexing association constants determined by UV and NMR methods show that N-substituted maleimides form more stable complexes with styrene than with ethylbenzene in organic media. Based on this result, new polymer membranes are developed to separate styrene from styrene/ethylbenzene by pervaporation. N-substituted maleimides are coupled to a glassy polymer backbone (poly vinylalcohol) as affinity groups to facilitate transport of styrene through the membrane. Separation efficiencies and mechanisms are studied through swelling ratios, desorption and pervaporation measurements.

Chapter 1
Introduction

1.1 Membrane processes

Separation, concentration and purification of molecular mixtures are significant problems in both academic and industrial chemical processes. Industrial and academic research efforts have developed a number of separation techniques including distillation, crystallization, extraction and chromatographic methods. More recently, a new class of membrane-based separation processes have been reported. Attractive features of these novel processes include: 1) low energy consumption; 2) ability to integrate membrane-based processes into modular separation systems; 3) continuous operation under mild conditions and 4) tunable membrane properties for a dynamic range of separations. These advantages make new membrane-based methods more favorable than standard, classical separation methodologies [1].

In membrane separation processes, a selectively permeable membrane is used as a physical barrier between two phases while restricting the transport of various chemical species across the membrane (Figure 1.1). Chemical species can be selectively transported across the membrane only when a driving force acts upon them. The feed phase is divided into two parts during contact with the membrane. The portion transferred across the membrane is termed "permeate" while the membrane-impermeable portion is called "retentate" (Figure 1.2) [1]. Separation is realized via differences in size, shape, vapor pressure, affinity, charge or other physical and chemical properties of the components in the mixture. Species discrimination by

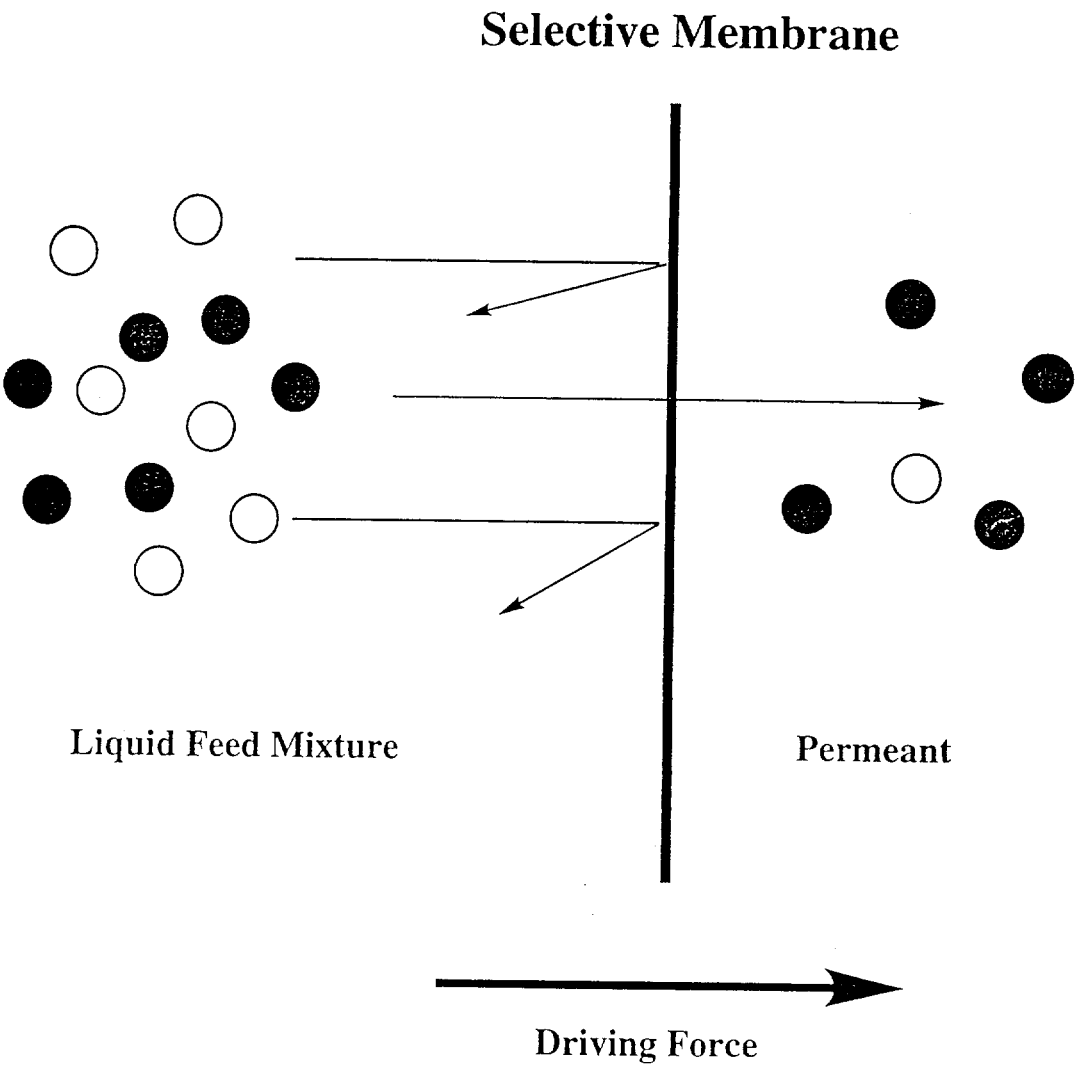

Figure 1.1 Schematic representation of a membrane separation process.

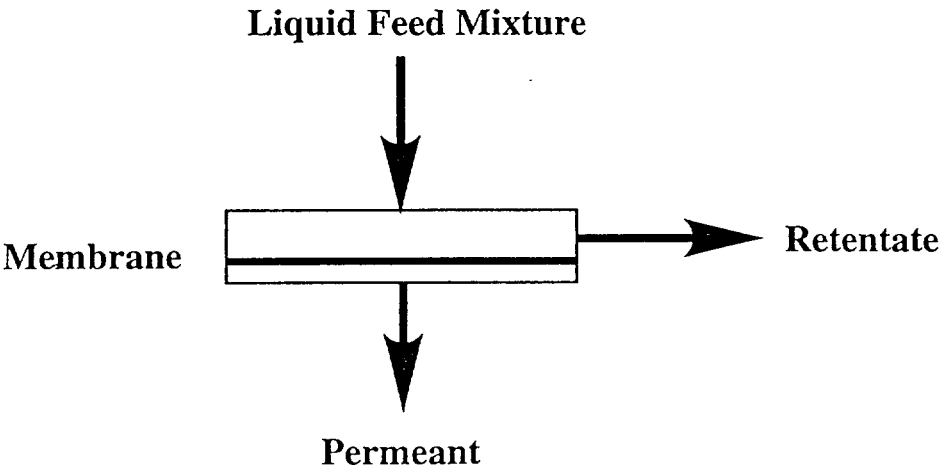

Figure 1.2 Schematic representation of a membrane process where the feed stream has been separated into a retentate and a permeate stream.

the membrane is the crucial step in achieving efficient separation. Membrane structure and function are the principal factors determining separation efficiency. In other words, the chemical and physical nature of the membrane determine the type of separation, ranging from the separation of microscopic particles to molecules with similar sizes and shapes.

1.1.1 Separation processes

To separate particles of different sizes and shapes using membrane processes, microporous membranes which have pore sizes ranging from less than 2 nm to 10 μm in diameter are usually used and the driving force for these processes is generally a pressure gradient across the membrane. Typical pressure-driven membrane processes are microfiltration, ultrafiltration, reverse osmosis and gas permeation. Microfiltration is applied to retention and oncentration of particles with diameters in the range of 100-

10,000 nm from a solvent or other components of low molecular weights. With microfiltration, it is possible to use membrane structures characterized by large heterogeneous pore sizes. Ultrafiltration is used to separate particles smaller than 100 nm in diameter. The membrane structure must be more dense and the applied pressure must be necessarily greater in this process. It is possible to separate even smaller particles using membranes with higher density and higher pressure. This process is referred to as hyperfiltration or reverse osmosis, because an osmotic pressure is established as the result of the difference in trans-membrane permeate concentration. In this case, the pressure applied must overcome the osmotic pressure. Then, solvent flux can be reversed so that the solution with greater concentration is further concentrated.

Microfiltration, ultrafiltration and reverse osmosis are fundamentally identical processes (Figure 1.3) [2]. Under the driving force of a hydrostatic pressure gradient, some components permeate through the membrane while others are retained, according to the size and shape complementarity of the components with the membrane pores. The separation mechanism is a sieving effect. Factors affecting separation efficiencies are largely related to disparities between the sizes of the particles to be separated and the membrane pores. In addition to these three membrane processes, gas permeation falls into the class of pressure-driven membrane processes where pressure is used as a driving force and, in this case, gas permeation is similar to reverse osmosis. The gas to be purified is enriched on the permeate side of the membrane against the partial pressure of this gas in the feed.

Gas permeation also falls into the class of **concentration** gradient-driven membrane processes. In addition, pervaporation, dialysis and liquid membranes are related to membrane processes utilizing concentration gradients as drivingforces. In these processes, homogeneous, dense polymer membranes are commonly used. The

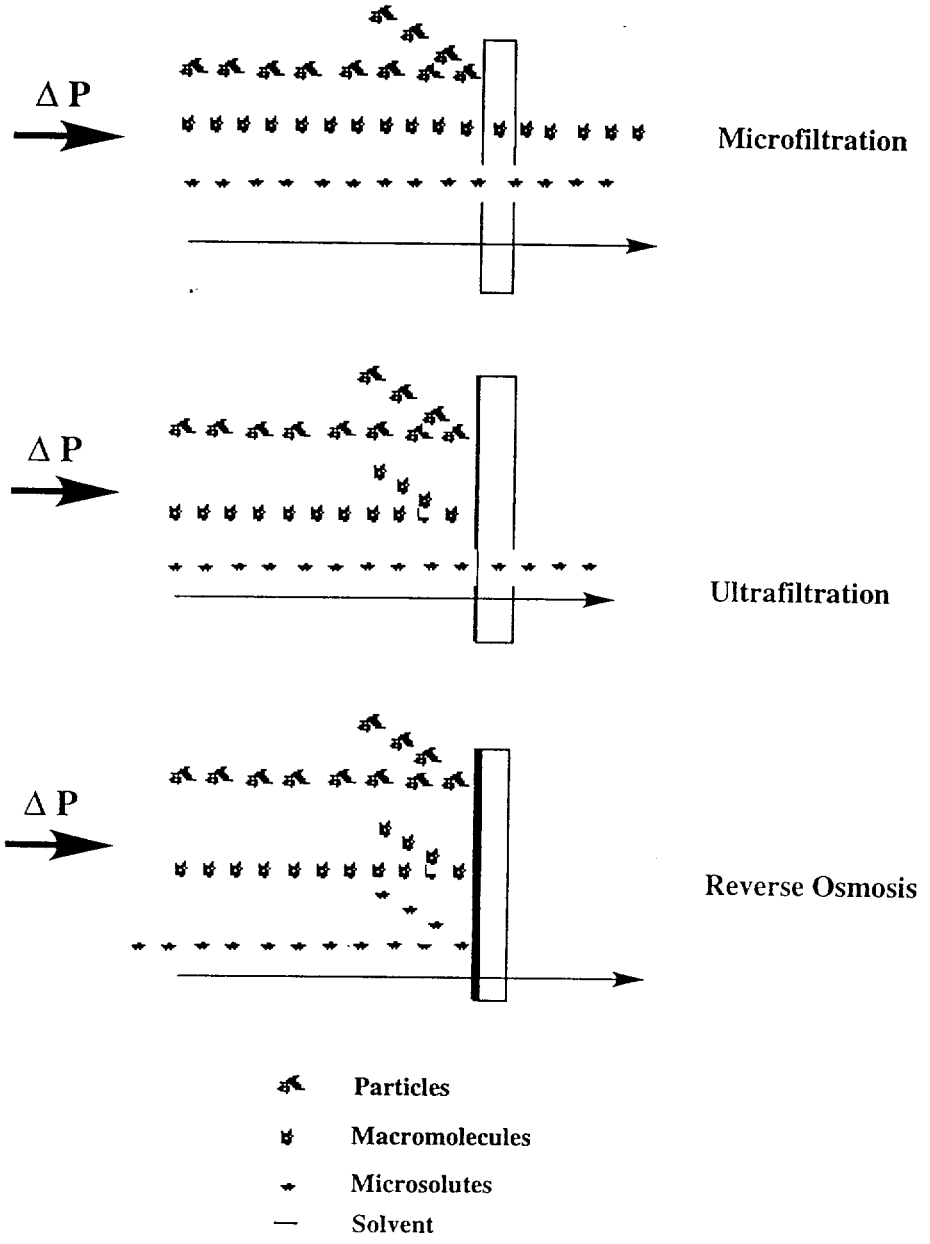

Figure 1.3 Schematic representation of pressure-driven membrane separation processes.

separation mechanism is based on the solubility and diffusivity of the various components in the membrane (Figure 1.4). Three steps are involved in mass transport across the membrane: 1) sorption of the various components from the feed mixture to the membrane; 2) diffusion of the components across the membrane according to the activity gradients of each component; and 3) desorption of the components from the membrane as permeate. In gas permeation, interaction between gas and the membrane is small, with the permeability and selectivity assumed to be governed by the intrinsic diffusivities of the gases in the membrane. In a related process termed "pervaporation", separation of liquid mixture is achieved while a phase transition occurs with the feed being a liquid and the permeate a vapor. Due to significant interactions between those liquid molecules and membrane components, the permeating liquid components within the membrane play an important role in determining the separation selectivity and permeability. Solubility of liquid components towards the polymer membrane is much higher and diffusion coefficients become concentration-dependent for this process.

An electrical potential gradient can also be used as a driving force for membrane processes [3]. Examples include electrodialysis, electrolysis, and also pervaporation. Electrically charged membranes and ionized permeate are required for these membrane processes.

1.1.2 Membranes

Membranes are principal and critical components in membrane-based separation processes. Membrane structures determine the application and efficiency of separation processes. Even though natural biomembranes provide a general architecture for highly selective, efficient transportation of species across a barrier, synthetic membranes normally used in actual, industrial separation processes are much less sophisticated and performance-limited.

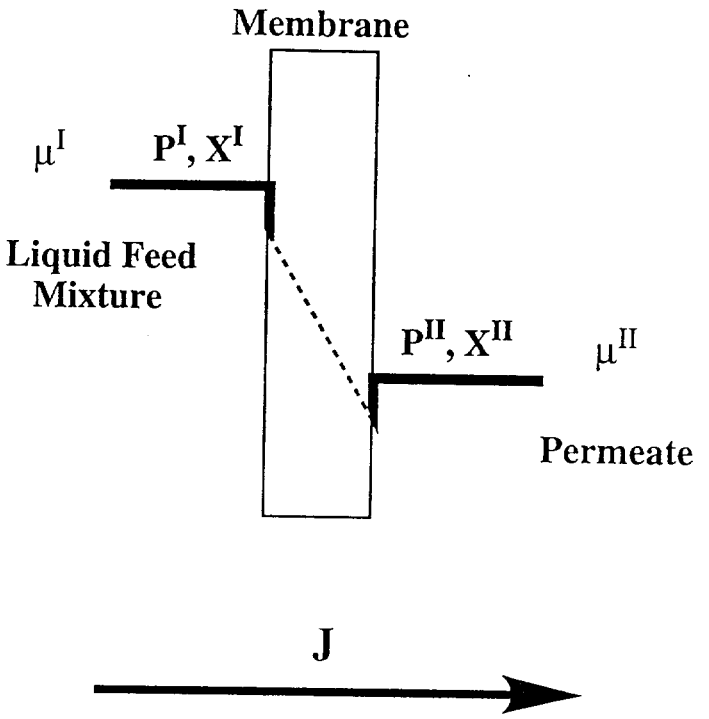

Figure 1.4 Schematic representation of the three-step solution-diffusion transport mechanism.

Utilizing different membrane morphologies and structures, separation processes can take advantage of microporous or homogenous films [1]. A membrane with microporous structure cnsists of a solid matrix with well-defined holes or pores. Pore diameter determines the permeability and selectivity of the membrane. A homogenous membrane is a dense polymer film through which a mixture of molecules is transported by a pressure, concentration or electrical potential gradient. Separation of the various components of a mixture is the result of the difference in the transport rates of each component within the membrane, which in turn is determined by the differences in

intrinsic and facilitated diffusivities and concentration gradients of these components.

Development of asymmetric membranes has brought membrane processes from academic scale model systems to large-scale industrial applications. An asymmetric membrane consists of a very thin, dense top-layer supported by a highly porous, thick supporting sublayer [1]. Selectivity and permeability are determined mainly by the thin dense top-layer. The porous sub-layer provides a support for the thin and fragile top-layer under pressure or other process requirements. It is also possible to fabricate composite, sandwich-type membranes in which different materials are used as top- and sub-layers.

1.1.3 Mass transport in membranes

Generally, permeability and selectivity are directly related to transport rates of molecules across membranes. Transport rates in turn are governed by driving forces acting on each component. In membrane processes, three general forms of mass transport can be distinguished: passive transport, facilitated transport and active transport (Figure 1.5) [1]. When a membrane acts only as a barrier through which all the components are transported under driving forces of a pressure, concentration or electrical potential gradient across the membrane, mass transport through the membranes is referred to as passive transport. Facilitated transport is a special form of passive transport. In this case, transport of the components is still dependent on the electrochemical potential gradient across the membrane, but is also facilitated by transport coupling to a specific carrier confined to the membrane as shown in Figure 1.5b. Active transport is the opposite of passive transport. Transport of the components occurs against the gradient of their electrochemical potential. An interaction between the component to be separated and specific carriers within the membrane provide the component with the energy to overcome the electrochemical potential across the

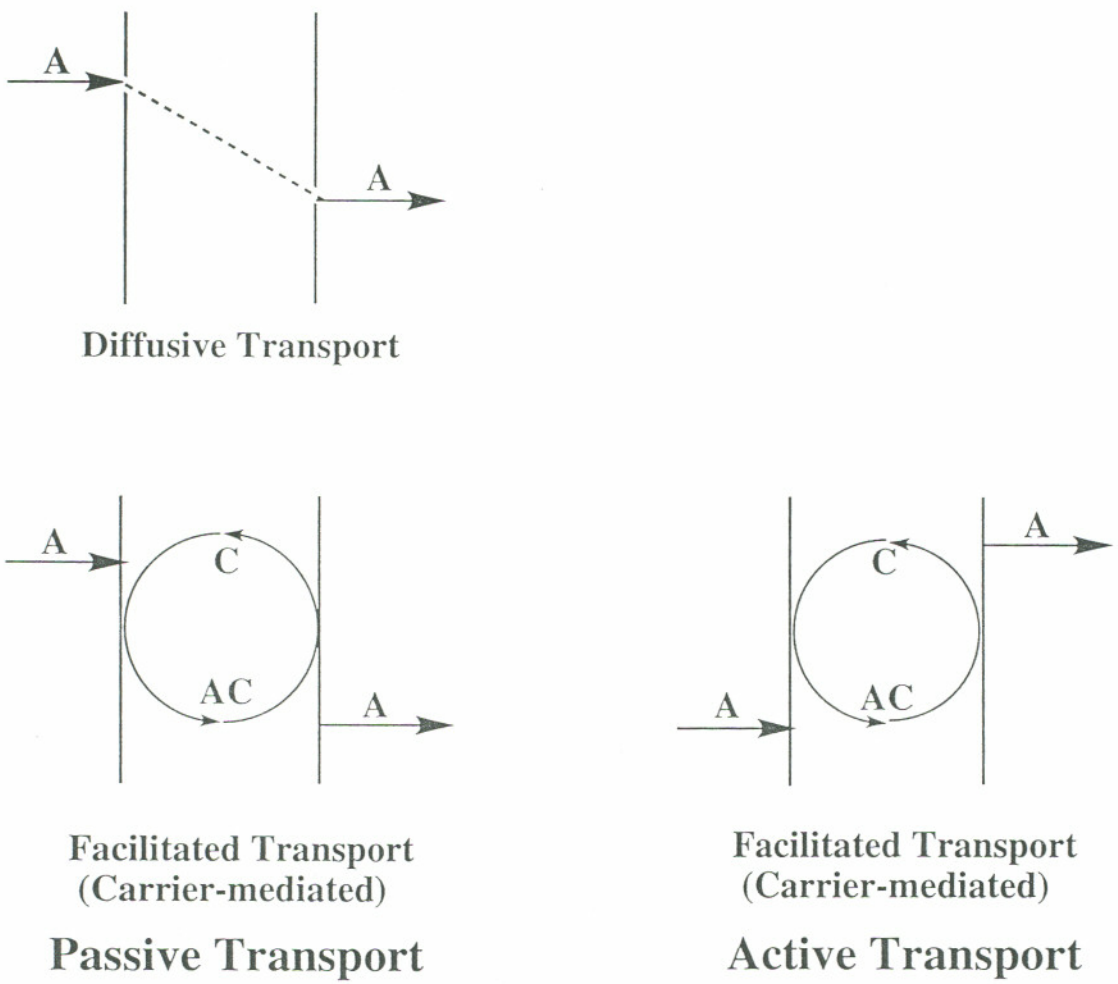

Figure 1.5 Schematic representation of the various forms of membrane mass transport.

membrane as they travel through the membrane.

Based on a phenomenological equation which relates membrane fluxes to their driving force, mass transport in various membrane processes has been mathematically modeled [4,2]. Transport equations for each membrane process are different, but in all membrane processes the permeant flux is inversely proportional to membrane thickness. In order to improve the transport rate in membrane processes, membranes need to be as thin as possible.

1.2 Pervaporation

Pervaporation is a membrane separation process in which permeate is selectively transported through a homogeneous, nonporous membrane with simultaneous permeate evaporation. It is a unique membrane process in that permeate undergoes a phase change from liquid to vapor during its transport through the membrane barrier [5]. In common with other traditional separation methods including extraction and distillation, liquid mixtures are separable using pervaporation. The features of low energy-consumption and high selectivity make pervaporation an attractive method for further development.

In pervaporation, selective mass transport through a membrane takes place when a driving force acts upon the feed mixture components. The driving force for pervaporation is a chemical activity gradient of the permeating components across the membrane, which is achieved by lowering the activity of the permeating components on the permeate side of the membrane.

Performance of the pervaporation membrane system is characterized by two parameters [6]: (1) permeability and (2) selectivity of the membrane towards different components in the mixture to be separated, both of which are governed by the solubility and diffusivity of each liquid component in the membrane. The permeability of a

membrane to a component, P, can be determined by a permeate flux, J, if the membrane thickness, l, is known.

$$J = \frac{P}{l} \qquad (1\text{-}1)$$

The permeate flux, J, is expressed as the weight of the permeate transported per unit time and membrane area.

$$J = \frac{W_P}{t \cdot A} \qquad (1\text{-}2)$$

where W_P is the weight of the permeate transported across the membrane, t and A are the time for transporting the permeate and the membrane area, respectively. The separation selectivity can be quantified by the separation factor, α, of the membrane defined as:

$$\alpha = \frac{(C_A/C_B)_P}{(C_A/C_B)_F} \qquad (1\text{-}3)$$

where $(C_A/C_B)_p$ is the concentration ratio of component A vs. component B in the permeate, and $(C_A/C_B)_f$ is the concentration ratio of component A vs. component B in the feed solution.

1.2.1 Mass transport mechanisms and pervaporation processes

In order to understand selective transport of liquid mixtures through membranes, various mechanisms have been proposed. Binning et al. [7] suggested a liquid permeation model in which a highly swollen, liquid-saturated zone and a gas zone coexist within the separation membrane. Here, selectivity takes place in the boundary layer between the liquid and gas zones. Another model used to explain pervaporative

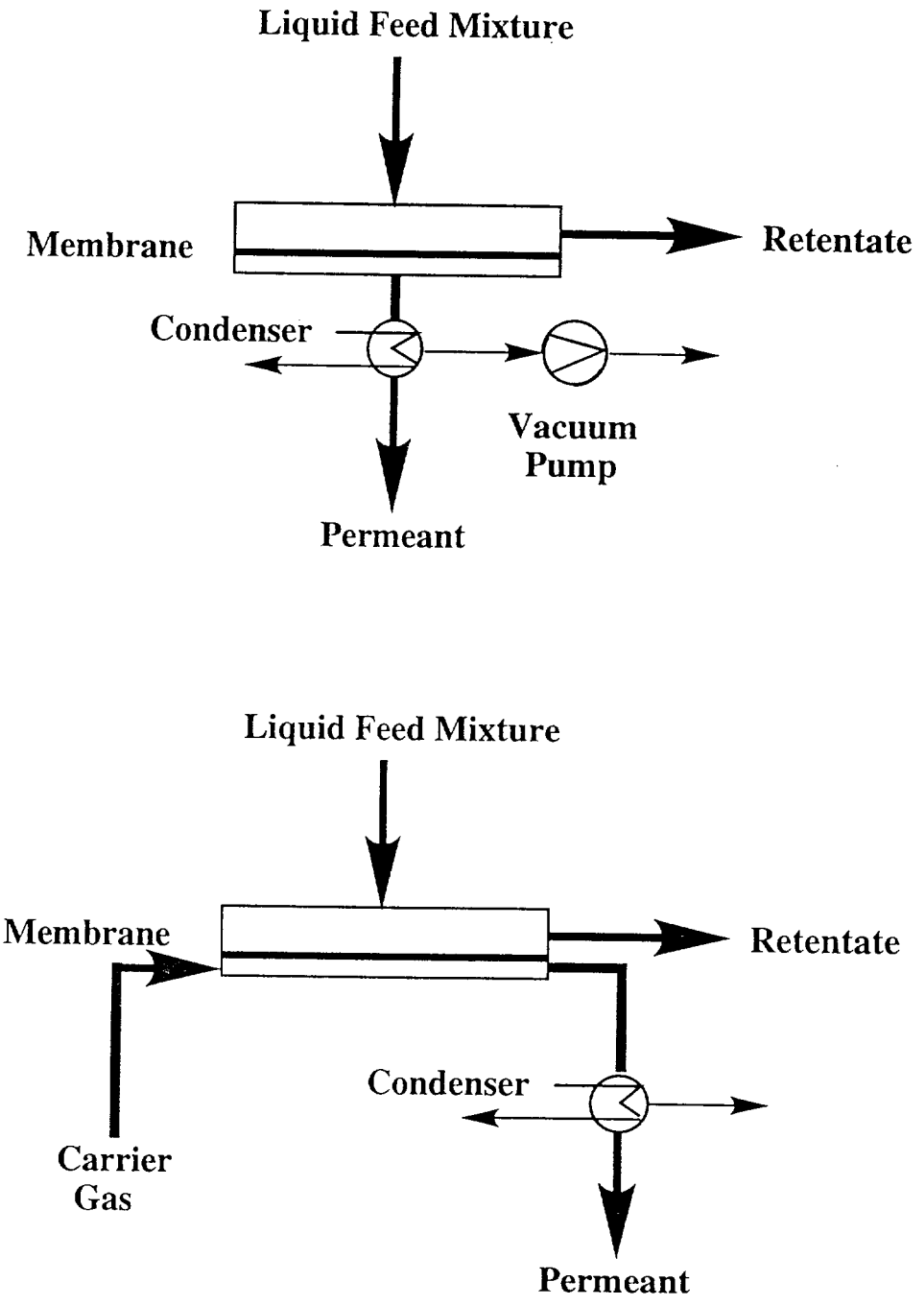

Figure 1.6 Schematic drawing of vacuum pervaporation and sweep-gas pervaporation

gradient and evaporate into the vacuum on the permeate side. Sweeping pervaporation uses a carrier-gas which circulates in countercurrent flow with respect to the process liquid mixture stream. Permeate is swept out of the membrane by the flow of carrier-gas and collected into a cold-trap by the flow of the permeated vapor loaded carrier-gas. The carrier-gas circulates continuously within the pervaporation module.

Membranes usually exhibit a relatively larger interaction with liquid and vapor as compared to gas. Unlike gas permeation, solubility of permeating liquid components in polymer membranes is generally very high in pervaporation. The high solubility also leads to a high diffusivity due to an increase of polymer segmental motion and free volume in the polymer membrane resulting from an increasing amount of plasticizing liquid permeate inside the membrane [14]. More rapid liquid component diffusion through liquid over solid polymer phases is another contribution to high diffusivity caused by high solubility. In this case, the diffusion coefficient of the permeating component becomes concentration dependent. Therefore, high permeabilities are achievable with pervaporation. High selectivity can also be obtained in pervaporation due to large differences in the membrane interactions with different liquid mixture components, leading to selective sorption of the component in the mixture to be separated into the membrane and selective diffusion across the membrane.

1.2.2 History of pervaporation

The phenomenon of pervaporation was first introduced in 1917 by Kober in the studies dealing with concentrating aqueous solutions enclosed in a collodion bag [15]. Following this preliminary study, several contributions were made on the removal of water from organic compounds using membrane processes. In particular, the group of Binning and coworkers [16, 17] made notable research contributions to the practical application of pervaporation to petrochemical industrial separations in the early 1960's.

A series of investigations were carried out on the separation of hydrocarbons using ethyl cellulose membranes and the removal of water from organic chemicals [18, 19]. Meanwhile, systematic research on transport and separation of liquid mixtures using permselective membranes, theories of transport and separation, and principles of pervaporation processes were reported by the groups of Michaels et al. [8], Long [20], Sweeny and Carter [21, 22], respectively. Nevertheless, research in this area was hampered until the early 1970's due to the lack of suitable membrane materials with sufficient selectivity, permeability and stability, which prevented pervaporation from competing with other traditional separation techniques. In the 1970's, the fossil fuel energy crisis directed research attention to alternative energy-saving separation techniques making use of membranes. Subsequently, progress in polymer chemistry and other membrane technologies greatly improved the feasibility of pervaporation-based separation processes.

1.2.3 Separations carried out by pervaporation

Separations accomplished by pervaporation is considered to be one of the most promising processes in energy-saving separation technology. Attention was first drawn to ethanol dehydration [23, 24, 25, 26, 27]. Various pervaporation membranes have been developed with permeability and selectivities high enough to be commercially viable. Dehydration of other organic solvents such as isopropanol [28, 29], dioxane [30], caprolactam [31] and acetone [32] have also achieved moderate success. Meanwhile, extensive studies were done on the removal of organic chemicals from diluted organic aqueous solution using elastomeric composite [33, 34, 35] and ion-exchange membranes [36, 24]. In recent years, separation of organic mixture using pervaporation has attracted more and more attention due to potentials of pervaporation to separate azeotropes, compounds with small differences in boiling characteristics or

other similar properties. Lower energy consumption also makes pervaporation methods more attractive for any type of separation.

1.3 Pervaporation using new polymer membranes incorporating complexing groups

Although the potential and advantages of pervaporation have been demonstrated by previous studies, this separation technique has not been put into practical use because of the delay in the development of the membranes with specific, selective permeabilities, especially for organic-organic mixture separations. After several decades of studies on the permeability and selectivity of polymer membranes, it has become clear that hydrophilic polymers appear to be the most suitable for dehydration of organic liquids [37]. The preferential sorption of water into hydrophilic polymer membranes allows water to diffuse readily through the membrane. Elastomers which preferentially absorb and permeate organic components are the most favorable materials for preparing membranes to remove organics from water [37]. Many strategies have been developed in designing specific membranes to improve the permeability and selectivity of the membranes towards certain mixtures. One strategy focuses on morphological designs of membranes [37]. Asymmetric and composite membranes offer the possibilityof making a membrane with a thin effective separation layer, which leads to an increasing permeability, and a porous sublayer to maintain mechanical strength. Other efforts have been made on adopting polymer materials with specific properties, or chemical and physical modification of polymer materials to drastically change their intrinsic properties. Sweeny et al. [21] reported that material polarity can be altered to improve separation efficiency. In the case of binary liquid mixtures consisting of components with different polarity, the component whose polarity most closely matches that of the membrane preferentially permeates.

Polymeric membranes with microphase separated structures have also been developed to enhance selectivity of the membrane [38]. Continuous phases of microdomains in which only a selective solvent can dissolve are formed to give permeating pathways to the selective solvent. The membrane displays favorable selectivity. Block and graft copolymers are generally used to form microphase separated structures due to the incompatibility of constituent chains. These microdomain structures depend on the composition of copolymers, the length of constituent chains, and casting conditions [39]. Separation of the selective solvent is effected by the morphology of membrane. Using this concept, separation of benzene-cyclohexane was achieved by employing a 2-hydroxyethyl methacylate (HEMA) (branch) - methyl acrylate (MA) (backbone) comb-type graft copolymer which was found to form a microphase separated structure [38]. Both benzene and cyclohexane are insoluble in oligo(HEMA), and benzene has a high solubility towards poly(MA). Also permselectivity of ethanol in separating ethanol from ethanol aqueous solution was accomplished by introduction of short polydimethylsiloxane (PDMS) chains into poly(1-trimethylsilyl-1-propyne) (PTMSP)[40, 41, 42]. A delicate alternating membrane structure was formed in this modified PTMSP membrane. Hydrophobicity of PTMSP membrane was increased by the introduction of short PDMS chains to improve ethanol solubility. Excellent permselectivity of ethanol was brought about by maintenance of high permeability of the original PTMSP membrane and improvement of ethanol solubility with short PDMS chain. The selectivity and permeability of the polymer material was optimized by adjusting the composition of the polymer membrane. Hydrogen bonding between permeants and membranes has also been utilized to improve membrane permeability and selectivity [43, 44].

Despite many attempts to develop polymer materials suitable for specific liquid mixture separations, and several examples of successful commercialization and

industrial application, organic-organic mixture separation still remains the most difficult issue to resolve, especially for those mixtures with similar molecular sizes, shapes or other physical and chemical properties. The selection rationale for choosing membrane materials for specific organic-organic separations is still unclear.

To achieve separation via membrane processes, membranes must be able to discriminate subtle differences between permeate molecular size, shape, or other physical and chemical properties. Also, membranes have been modified with functional groups which have specific interactions with feed components to facilitate separation. In the latter case, both selectivity and permeability of membranes towards a specific component should be naturally increased as a result of the recognition event between permeate components and membrane functional groups. Such an approach has been reported in a liquid membrane system (Figure 1.7) [45, 46]. A functional compound termed a "carrier" exists within the liquid separation membrane. Facilitated permeate transport through the liquid membrane relies on the reversible formation of a specific carrier-permeate complex. Permeability and selectivity of a facilitated transport membrane is dependent primarily onthe strength of the complexation. The carrier-permeate complex should be strong enough to facilitate the selective transport of the specific component and weak enough to release the component on the downstream side of the membrane.

The reversible complexation of olefins by aqueous Ag^+ ions has been applied to olefin separation via liquid membrane technology using Ag^+-exchange carriers [47]. Based on the same strategy, a novel synthetic polymer membrane with functional groups as carriers for transport has also been designed (Figure 1.8) [48]. A complexing agent which selectively and reversibly interacts with the permeant of interest is incorporated into a relatively impermeable polymer membrane. The specificity of the interaction improves selectivity and provides an additional path for transport leading to

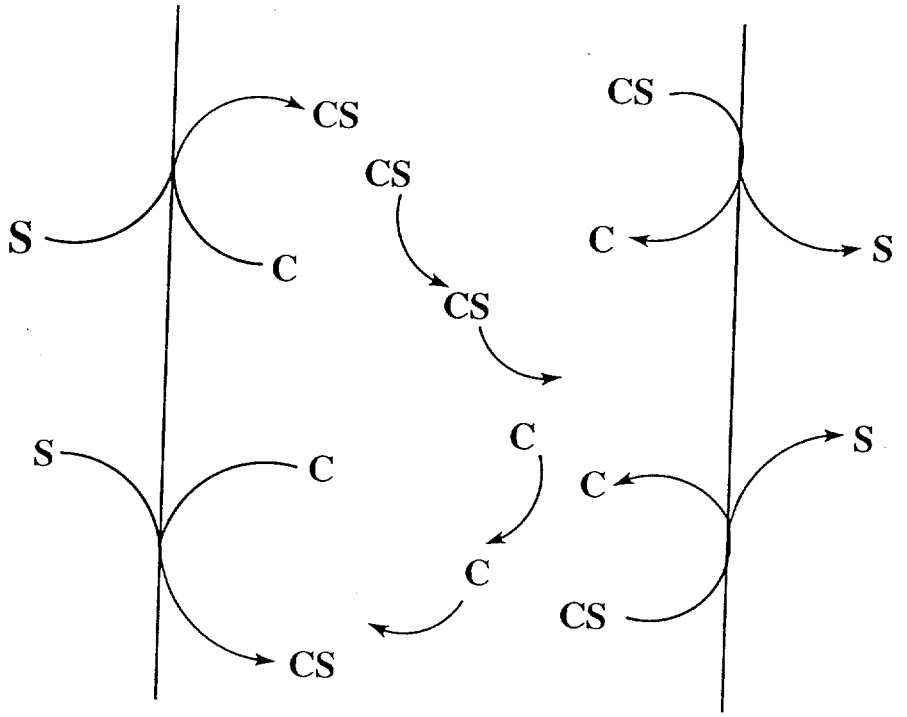

Figure 1.7 Schematic representation of facilitated transport in a liquid membrane containing reactive carrier.

high permeability of the membrane towards the specific compound.

Electron charge-transfer interaction has also been recently adopted as a specific interaction in the design of novel affinity-based complexing pervaporation membranes to separate styrene/ethylbenzene and aromatic/ aliphatic mixtures (Figure 1.9). Separation of styrene/ethylbenzene is of commercial interest because most styrene used in the production of polystyrene is prepared by catalytic dehydrogenation of ethylbenzene [47] and it remains one of the top ten distillation separation systems, consuming half the energy of all industrial distillation processes [49].

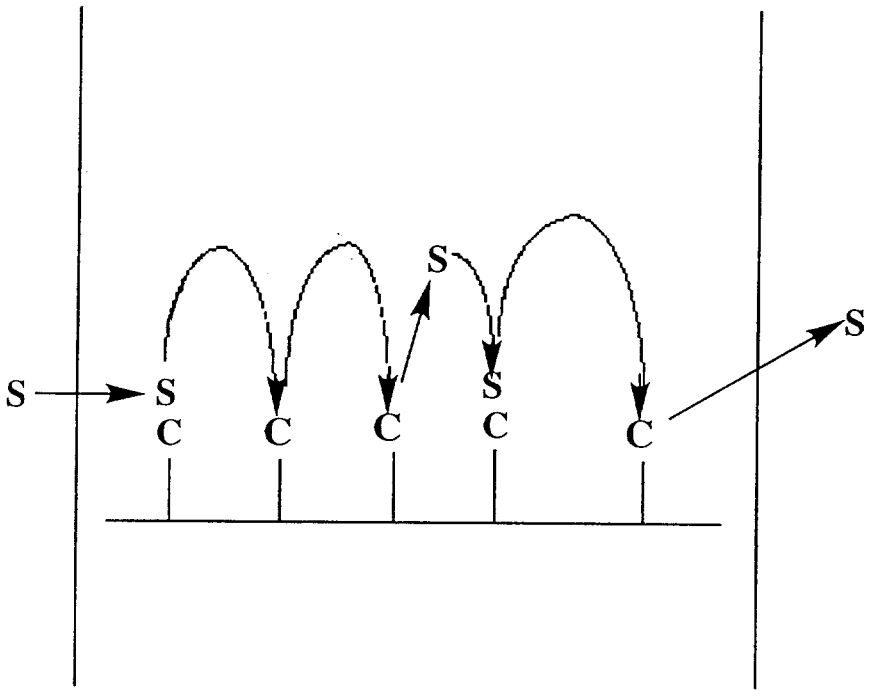

Figure 1.8 Schematic representation of transport in affinity-based complexing separation membranes.

Besides providing a new strategy to solve practical separation problems by the introduction of affinity groups into polymer membranes, affinity-based complexing pervaporation systems also permit further understanding of mass transport mechanisms by influencing specific membrane-permeant interactions and resulting transport selectivity and efficiency.

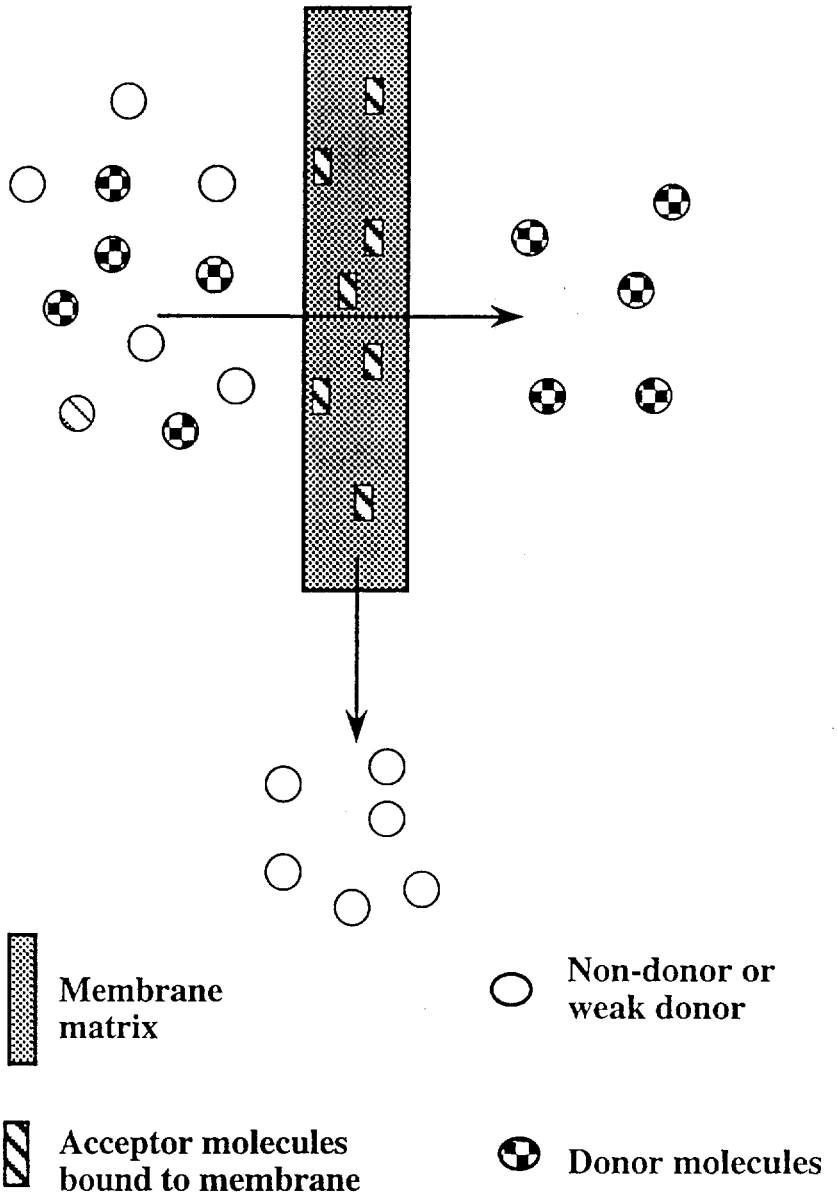

Figure 1.9 A novel membrane separation process based on electron charge transfer complexation.

1.4 Research objectives

The research described in this thesis provides a foundation for studies regarding new affinity-based pervaporation systems. Model electron accepting compounds are synthesized for complexation studies between model electron donating and electron accepting compounds and coupled to a glassy polymer backbone. Maleimide-based functional groups serve as model electron accepting compounds. Styrene/ethylbenzene mixtures serve as model electron donating permeating compounds. Phthalimide- and tetrachlorophthalimide-based compounds are used to investigate the influence of electron-donating groups and electron accepting groups attached to model electron accepting compounds on the strength of the charge-transfer complexation.

Research on molecular complexation between model electron accepting compounds and styrene/ethylbenzene is conducted to provide evidence for facilitated mass transport in a model affinity-based pervaporation system. Different strengths between styrene and ethylbenzene complexing with maleimide-based electron accepting compounds were evaluated in order to study the separation of styrene from the styrene/ethylene mixtures. Electron accepting compounds are coupled to partially hydrolyzed poly(vinyl alcohol) in model membrane systems for studying facilitated permeate mass transport through tailor-made derivatized polymer membranes for pervaporation.

Membrane swelling studies and separation evaluation will eventually be performed in a home-built pervaporation cell. The percentage of model accepting compounds coupled to polymer backbone will be adjusted to optimize the separation efficiency and investigate the influence of complexation on permeate permeability and selectivity within electron acceptor-derivatized pervaporation membranes.

Chapter 2
Model Electron-Donating and Electron-Accepting Compounds
Synthesis and Characterization

2.1 Introduction

Complexation between organic molecules occurs primarily through weak interactions between electron-rich and electron-deficient molecules. For over 100 years organic charge-transfer complexes have been studied. The influence and utility of this interaction has been applied in many chemistry related problems of fundamental and applied nature. In the simplest case, Lewis acid-Lewis base interaction relies upon electron transfer between two molecules, one of which is electrophilic while the other is nucleophilic [50]. Charge-transfer complexes have also been regarded as reaction intermediates in organic reactions such as the Diels-Alder reaction [51]. During the formation of such a cycloaddition of colorless products, a transient color formation is frequently observed to occur. This is ascribed to formation of chromic diene-dienophile complexes as intermediates. Alternating copolymerization of maleic anhydride with styrene is characteristic of the influence of charge-transfer complexation [52] . The formation of a 1:1 charge-transfer complex between maleic anhydride and styrene may participate in the polymerization propagation step, which leads to a well-controlled, alternating copolymer.

Formation of maleic anhydride-styrene complexes with a 1:1 stoichiometry ratio has been confirmed by the observation of the characteristic ultraviolet (UV) absorption spectrum [53]. In the UV absorption spectra of maleic anhydride in various solvents, the

absorption curves in aliphatic solvents are all very similar though not identical. This variation is ascribed to a solvent effect. UV absorption behavior of maleic anhydride in aromatic solvents is strikingly different from that in aliphatic solutions. In aromatic solvents, optical absorption of maleic anhydride is greatly intensified. A progressively bathochromic shift of the low energy absorption shoulder with increasing alkyl substitution of aromatic ring was observed (Figure 2.1) [54]. Especially in styrene, there is a marked bathochromic displacement of the absorption.

A structure for maleic anhydride-aromatic solvents has been proposed as the double bond of maleic anhydride is centrally located above two carbons para to each other across the aromatic ring [51]. Complexation between maleic anhydride and

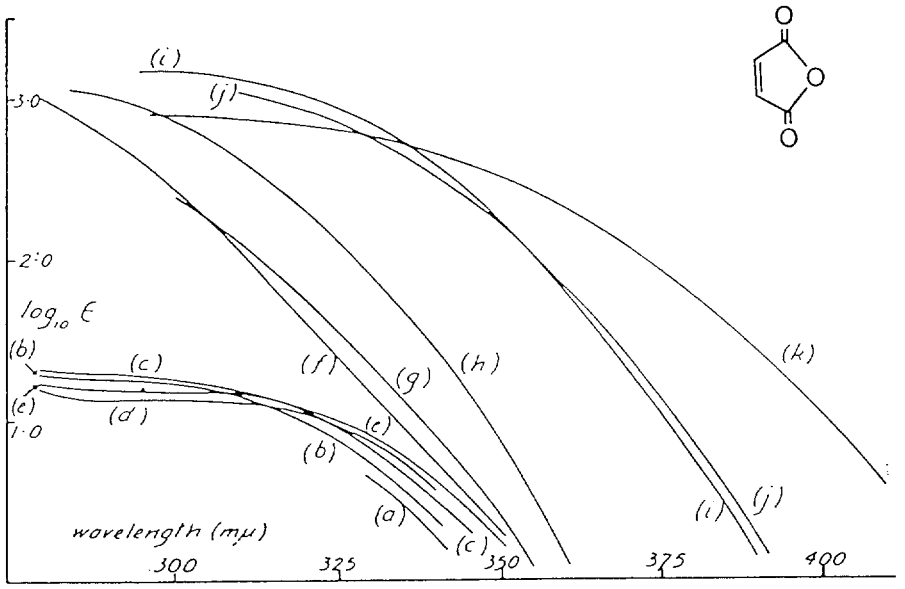

Figure 2.1 UV absorption of maleic anhydride in various solvents.
a) acetone, b) ethyl acetate, c) $CHCl_3$, d) hexane, e)CCl_4,
f) benzene, g) o-dichlorobenzene, h) toluene, i) mesitylene,
j) styrene, k)anisole; room temperature.

aromatic compounds could be described as a resonance hybrid based on a contribution characterized by electron transfer from the aromatic ring to maleic anhydride through such a structure (Figure 2.2). To eliminate the possibility that maleic anhydride-aromatic compound complex formation is due to selective coordination of the anhydride component with the aromatic ring, succinic anhydride, which lacks the double bond in a structure similar to maleic anhydride, has been employed to clarify the necessity for maleic anhydride's double bond for binding.

Complexation phenomenon of maleic anhydride with aromatic compounds and differences in complexation strengths of maleic anhydride towards styrene and other aromatic compounds has led to development of a model affinity-driven pervaporation system using maleic anhydride-based compounds as membrane-resident functional groups. Maleic anhydride-based compounds interact with styrene and other aromatic compounds through a charge-transfer mechanism to facilitate separations of styrene/ethylbenzene and aromatic/aliphatic mixtures. As multi-component mixtures interact with the membrane, complexes are formed between maleic anhydride-based groups coupled with the polymer membrane and aromatic electron-donating species in the mixture. Each aromatic compound has a characteristic binding constant with the electron-accepting groups on the membrane. Based on these differences, separation of aromatic or aromatic/aliphatic mixtures may be possible because components with larger complexation constants are transported more rapidly in the affinity-based membrane. Reasons for this are discussed more fully in chapter 5.

Partially hydrolyzed poly(vinyl alcohol) was chosen as the polymer membrane component. Maleic anhydride was converted to N-benzoyl chloride substituted maleimide to be coupled to poly(vinyl alcohol). The corresponding succinic anhydride-based compound, N-benzoyl chloride substituted succinimide lacking the double bond in maleimide responsible for complexation with membrane-resident

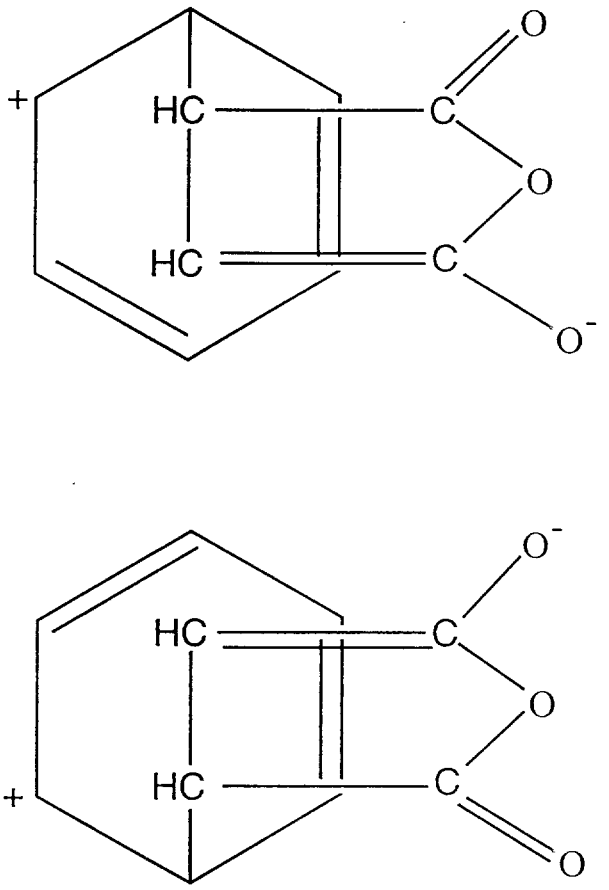

Figure 2.2 Proposed resonance hybrid structure for the benzene-maleic anhydride complex

maleimide groups, was also synthesized. Maleimide groups function as electron acceptors to coordinate with aromatic species. Complex stabilities can be adjusted with substituents which alter the electron density of maleimide groups. Several structurally similar model electron-accepting compounds, such as N-benzoyl chloride substituted phthalimide and tetrachlorophthalimide, were synthesized to adjust complexing strengths by placing electron withdrawing groups around the imide ring.

2.2 Experimental methods

All products synthesized were characterized by NMR and melting point determination.

Proton nuclear magnetic resonance (NMR) spectra were obtained on a 300MHz-GE spectrometer. Proton chemical shifts are expressed in parts per million (ppm) referenced against tetramethylsilane (TMS) standard.

Melting points of the compounds were determined in one of two ways: visual observation of sample melting via MEL-TEMPII melting point apparatus in the open capillary tubes or measuring enthalpies of melting by differential scanning calorimetry (DSC).

2.2.1 Reagents and solvents

Most reagents and solvents were obtained from Aldrich Chemical Co. The following reagents and solvents were used without further purification: 4-aminobenzoic acid, phthalic anhydride, tetrachlorophathalic anhydride, acetic anhydride, succinic acid, thionyl chloride, deuterated chloroform and dimethyl sulfoxide-d_6.

The following reagents and solvents were purified using standard procedures: maleic anhydride was recrystallized from chloroform. N,N-dimethylacetamide was shaken with BaO for several days, refluxed with BaO for 1 hour, then distilled under

reduced pressure. Chloroform was washed with water, dried with $CaCl_2$, refluxed with $CaCl_2$ and distilled.

2.2.2 Model electron-donating and electron-accepting compounds

Styrene, ethylbenzene, cyclohexane served as model electron donating compounds. Electron-accepting compounds were designed and synthesized based on various anhydride as described below. Corresponding succinic anhydride-based compounds were synthesized for comparison.

2.2.2.1 4-maleimidebenzoic acid (MIBA)

35.28 g of 4-aminobenzoic acid (0.259 mol) was added to a 250-ml three-neck, round-bottom flask with 100 ml DMAc and partially dissolved. The solution was stirred magnetically while a clear solution of 25.23 g maleic anhydride (0.257 mol) in 20 ml DMAc was added dropwise. Immediately, formation of a yellow solution with some undissolved 4-aminobenzoic acid was observed. After stirring the solution for 22 hours, 4-aminobenzoic acid finally dissolved. 5 g of NaOAc was added to this solution with 42.5 ml of $(AcO)_2O$ and partially dissolved into solution. The solution was stirred magnetically at room temperature for 24 hours while NaOAc totally dissolved, followed by the formation of a light brown solution. At this time, the temperature of the solution was increased to 65°C for 4.5 hours while stirring the solution magnetically. The color of the resulting solution changed from light brown to dark brown. This solution was cooled to room temperature and some DMAc in the solution was removed using a rotary evaporator. The concentrated solution was poured into 400 ml of cold water, and a light brown precipitate formed immediately. The precipitate was suction filtered and washed several times with water, then dried overnight in a vacuum oven. Recrystallization from acetone twice yielded white crystals (yield 37%) with mp 237.0-238.5°C.

^{1}H-NMR (aceton-d_6, ppm) δ 7.09 (s, 2H, vinyl-H in maleimide), 7.58 (d, 2H, Ar-H ortho to -COOH), 8.15 (d, 2H, Ar-H ortho to imide).

2.2.2.2 4-maleimidobenzoyl chloride

To a 100-ml one-neck round bottom flask, 6.64 g of 4-maleimidobenzoic acid (0.03 mol) and excess of thionyl chloride (about 30ml) were added. 4-maleimidobenzoic acid was stirred in thionyl chloride for 24 hours at room temperature and remained partially dissolved. Increasing the temperature to 55°C promoted dissolution of 4-maleimidobenzoic acid into thionyl chloride, followed by gradual formation of a clear, light yellow solution. The solution was stirred at 55°C for 3.5 hours. Then, excess thionyl chloride was distilled away under reduced pressure, with the protection of desiccant and gas absorption trap. After removing excess thionyl chloride, the whole distillation system was kept under the reduced pressure for 3 hours to ensure all remaining thionyl chloride was removed. A light yellow solid product was obtained. Recrystallization from a mix of chloroform-toluene, resulted in a needle-like, off-white crystals (yield 67%), mp 167-169°C.

^{1}H-NMR (chloroform-d_1, ppm) δ 6.94 (s, 2H, vinyl-H in maleimide), 7.65 (d, 2H, Ar-H ortho to -COCl), 8.22 (d, 2H, Ar-H para to -COCl).

2.2.2.3 Succinic anhydride

3 g of succinic acid (0.025 mol) and 5.2 g of acetic anhydride (0.05 mol) were added to a 50-ml round bottomed flask with a reflux condenser protected by a calcium chloride drying tube. Gentle reflux of the mixture with a oil bath and magnetic stirring yielded a clear solution after one hour. Then, solution refluxing was continued and stirred for another hour to ensure completion of the reaction. The solution was then cooled to room temperature. While cooling, crystal formation was observed in the solution. The solution was sealed and placed in a refrigerator, resulting in complete

succinic anhydride crystallization from the solution. The product was collected on a Buchner funnel and washed with anhydrous ether and dried in a vacuum oven. Yield is 90%, mp 119-121°C.

2.2.2.4 4-succinimidobenzoic acid

Synthesis of 4-succinimidobenzoic acid was carried out using the same procedure employed for 4-maleimidobenzoic acid. Briefly, condensation of succinic anhydride with 4-aminobenzoic acid was followed by cyclodehydration using acetic anhydride and sodium acetate. Product was purified by recrystalization from acetone. Yield: 51.3%, mp 238-241°C.

^{1}H-NMR (chloroform-d_1, ppm) δ 2.8 (s, 4H), 7.4 (d, 2H), 8.2(d, 2H).

2.2.2.5 4-succinimidobenzoyl chloride

Conversion of 4-succinimidobenzoic acid to the corresponding acyl chloride was achieved by heating the acid with thionyl chloride. Conditions were similar to the synthesis of 4-maleimidobenzoyl chloride described in section 2.2.2.2. Recrystalization from 2:1 toluene/chloroform provides white needle crystals. Yield: 87%, mp 203-205°C.

2.2.2.6 Other model electron-accepting compounds

4-Phthalimidobenzoic acid, 4-tetrachlorophthalimidobenzoic acid and corresponding acyl chlorides were synthesized and purified based on analogous strategies as described above. Melting point for these compounds are 266°C(PIBC), 238°C(TCPIBC), 370°C(TCPIBA) and 288°C(PIBA).

2.3 Results and Discussion

Conversion of maleic anhydride to 4-maleimidobenzoyl chloride is accomplished by two reactions (Scheme 2.1). First, maleic anhydride is converted to 4-maleimidobenzoic acid by amidation to form amic acid followed by a fast ring-closing cyclization [55]. Then, the corresponding acid chloride was prepared using thionyl chloride. 4-maleimidobenzoic acid is barely soluble in chlorinated solvents and completely insoluble in aromatic solvents. In contrast to the precursor acid, the acid chloride is soluble in chlorinated solvents.

Other similar compounds were synthesized using similar protocols. Solubilities of PIBA and TCPIBA are poor in most solvents, even highly polar solvents such as DMF, DMAc and DMSO. PIBC and TCPIBC are slightly soluble in chlorinated solvents.

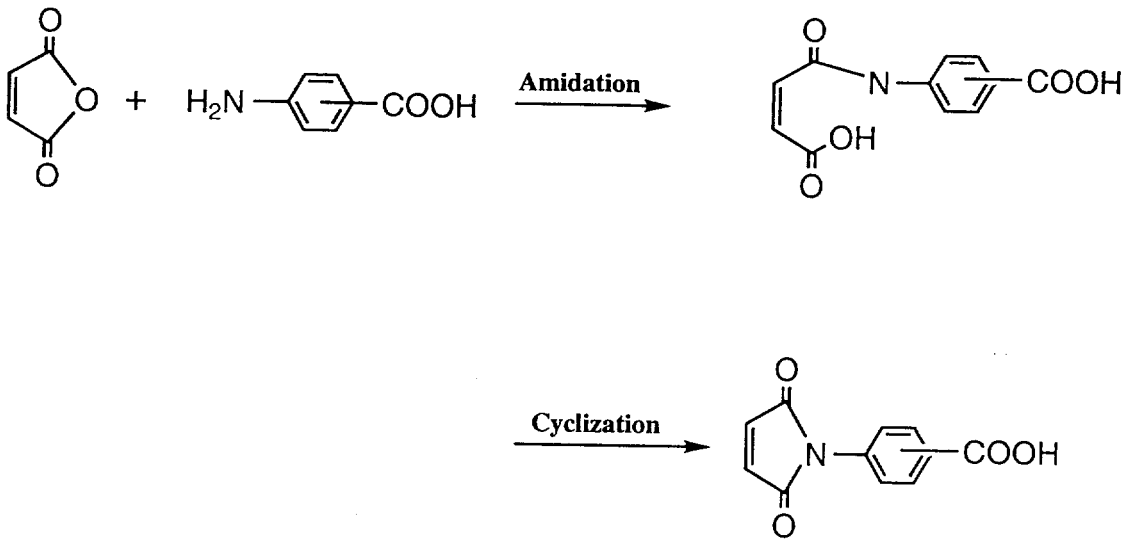

4-maleimidobenzoic acid (MIBA)

(1)

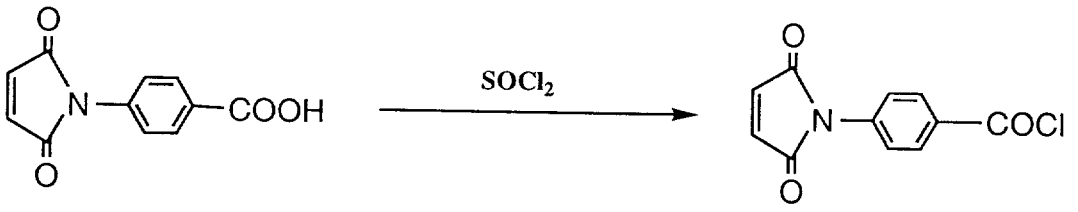

(MIBC)

(2)

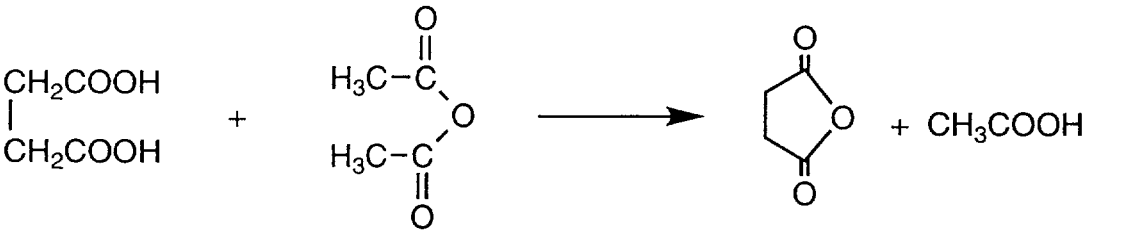

(3)

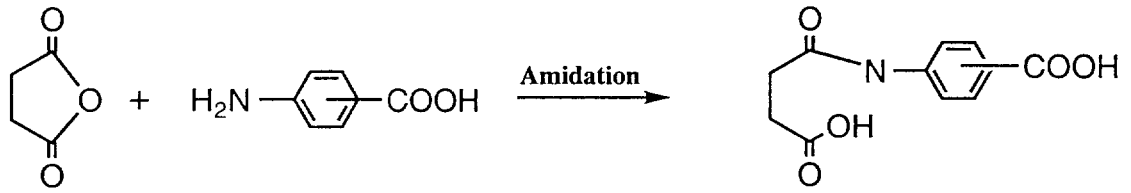

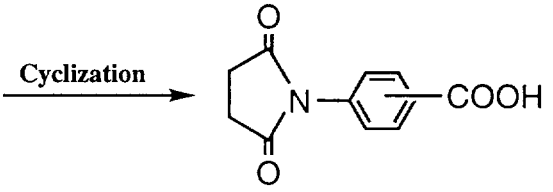

(4)

4-succinimidobenzoic acid (SIBA)

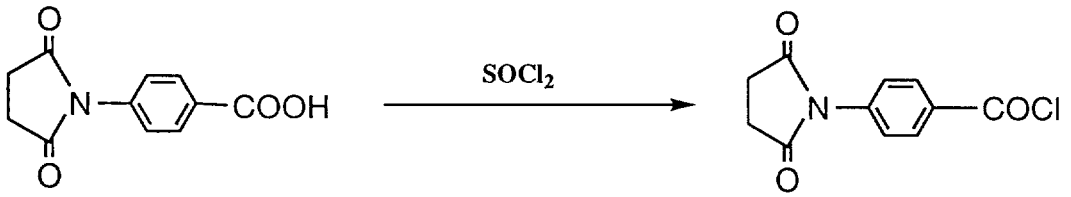

(5)

(SIBC)

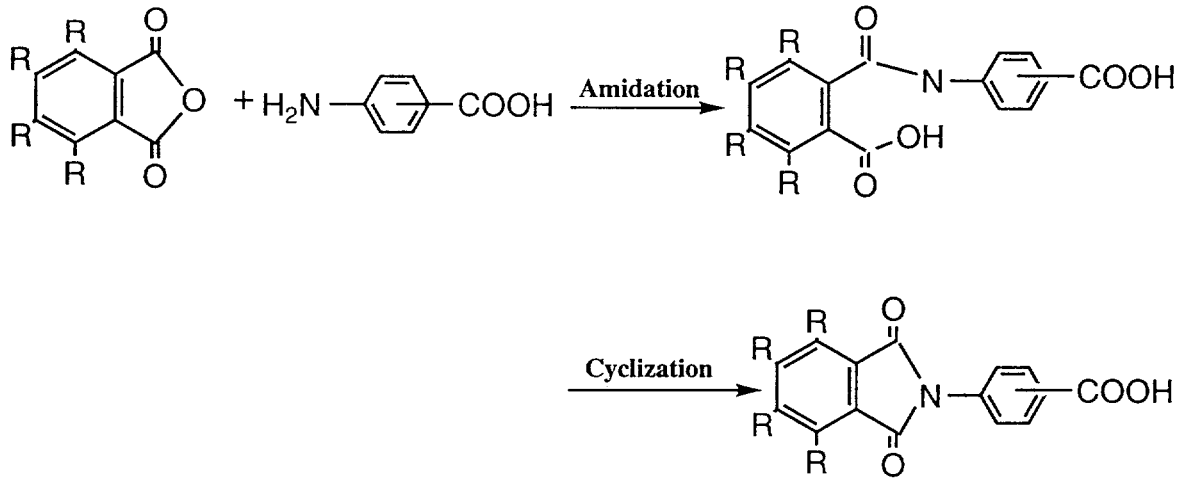

(6)

R= H, phthalimidobenzoic acid (or benzomaleimidobenzoic acid, PIBA)
= Cl, tetrachlorophthalimidobenzoic acid (or tetrachlorobenzo maleimidobenzoic acid, TCPIBA)

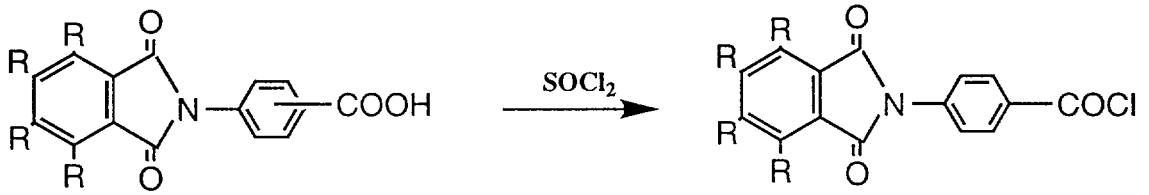

(7)

R=H, PIBC

=Cl, TCPIBC

Scheme 2.1 Synthetic route of model electron-accepting compounds

Chapter 3

Organic Charge-Transfer Complexation Studies between Model Electron-donating Compounds and Electron-accepting Compounds

3.1 Introduction

Molecules interact to varying degrees via both inter- and intra- molecular interactions. Generally, dispersion-related intermolecular interactions are small compared with interatomic forces within molecules manifested as covalent or ionic bonding. However, certain interactions between molecules are sufficiently strong to make it impossible to describe them simply in terms of dispersion and dipole-related forces. Molecular complexation is a phenomenon in which interactions between molecules are weaker than intramolecular forces, but stronger than any dispersion-related forces.

Organic charge-transfer complexes are formed by weak interactions between organic electron donating and accepting species. Dispersion, dipole-related forces together with charge-transfer interactions due to transfer of electrons from donor to acceptor components in complexes dominate energies of interactions between electron donors and electron acceptors [56]. As evidence for such interactions, the electronic absorption spectrum of a D-A complex exhibits several distinct characteristics [57]. These new profiles are characterized in terms of an intermolecular charge transfer transition involving electron transfer from the donor to the acceptor.

Charge-transfer complex absorption characteristics in solution may not be readily observed, as the complex is in equilibrium with constituent free donor and

acceptor species. In general, the spectrum of the complexing solution contains one or more absorption bands characteristic of the complex together with the individual absorption of both the free electron donating and electron accepting components. The position of the complexation equilibrium was first determined by Benesi and Hildebrand in their investigation of the interaction of iodine with aromatic hydrocarbons by measuring the intensity of the absorption of the charge-transfer complex solution [58]. Organic charge transfer complexes have a characteristic absorption that generally appears as a separate band red-shifted relative to the uncomplexed monomers.

In the Benesi-Hildebrand formulation, evaluation of the degree of association by measurement of the absorption of the complexing solution is based on the assumption that only a single complex species with definite stoichiometry (1:1) is formed, although the interaction of an electron donor with an electron acceptor may give rise to more than one species of complex in the solution. The equilibrium,

$$A + D \rightleftharpoons AD \tag{3-1}$$

is established, with the thermodynamic equilibrium constant, K_C^{AD}, written as

$$K_C^{AD} = \frac{[AD]}{[A][D]} = \frac{[AD]}{([D]_0 - [AD])([A]_0 - [AD])} \tag{3-2}$$

where [AD], [A] and [D] represent equilibrium concentrations of the complex AD and free components A and D, respectively. $[D]_0$ and $[A]_0$ indicate the initial concentrations of D and A, which includes concentrations of free and complexed D and A, respectively. Equation (3-2) may be rearranged to

$$\frac{[A]_0}{[AD]} = \frac{1}{K_C^{AD}} \cdot \frac{1}{[D]_0} + \frac{[A]_0}{[D]_0} - \frac{[AD]}{[D]_0} + 1 . \tag{3-3}$$

When measured absorptions are due entirely to the complex AD, the intensity of the absorption, according to Beer's law, for a 1-cm path-length of solution is

$$A = \epsilon_\lambda^{AD} \cdot [AD] \tag{3-4}$$

ϵ_λ^{AD} is the molar absorptivity of the complex AD at the wavelength of measurement. Then equation (3-3) becomes

$$\frac{[A]_0}{A} = \frac{1}{K_C^{AD}\cdot\epsilon_\lambda^{AD}}\cdot\frac{1}{[D]_0} + \frac{[A]_0}{[D]_0\cdot\epsilon_\lambda^{AD}} + \frac{1}{\epsilon_\lambda^{AD}} - \frac{[AD]}{\epsilon_\lambda^{AD}\cdot[D]_0} \qquad \textbf{(3-5)}$$

When the measurement is performed under conditions where $[D]_0 >> [A]_0$, the second and the fourth terms on the right-hand side of equation can be omitted. The Benesi-Hildebrand equation for determining the equilibrium position of the weak interaction is thus obtained as

$$\frac{[A]_0}{A} = \frac{1}{K_C^{AD}\cdot\epsilon_\lambda^{AD}}\cdot\frac{1}{[D]_0} + \frac{1}{\epsilon_\lambda^{AD}} \qquad \textbf{(3-6)}$$

Use of the Benesi-Hildebrand equation assumes that optical absorptions in the region of measurement are due entirely to the absorption of the complex AD when the initial concentration of D is much larger than that of A ($[D]_0 >> [A]_0$). For the system where the acceptor undergoes significant optical transitions and exhibits absorptions in the region of measurement, a new relationship must be derived from the Benesi-Hildebrand formalism. An equation derived by Ketelaar and co-workers can be used to evaluate K_C^{AD} in this case [59],

$$\frac{1}{\epsilon_\lambda^a - \epsilon_\lambda^A} = \frac{1}{K_C^{AD}(\epsilon_\lambda^{AD} - \epsilon_\lambda^A)}\cdot\frac{1}{[D]_0} + \frac{1}{\epsilon_\lambda^{AD} - \epsilon_\lambda^A} \qquad \textbf{(3-7)}$$

ϵ_λ^A ,ϵ_λ^{AD} are the molar absorptivity of uncomplexed and complexed acceptor, respectively. ϵ_λ^a is the apparent molar absorptivity which is obtained experimentally from the observed absorbance, A. The observed absorbance is the result of combining absorbance due to complexed and uncomplexed acceptor. Several assumptions are made in this case as well. Simple complexes are formed with definite stoichiometry (1:1). Additionally the initial concentration of donor is in large excess compared to that

of acceptor. Also, the contribution of donor to absorptions in the region of measurement can be compensated for by using a solution containing the same amount of donor with the complexing solution as a reference.

Determination of the association constant of the charge-transfer complex using nuclear magnetic resonance methods is also feasible. A method analogous to the Benesi-Hildebrand method was developed to evaluate the complexing equilibrium constant by Hanna and Ashbaugh [60].

Consider a chemical shift of protons on molecule A which are undergoing rapid exchange between the complexed and the uncomplexed state in the equilibrium shown in equation (3-1). The observed chemical shift of these protons will not be identical to the chemical shift of complexed or uncomplexed species. It will represent a time-averaged result of proton behaviors in different environments. Treatments used in NMR studies of hydrogen-bonding equilibria have been applied to observed chemical shifts of protons in complexing media [61],

$$\delta^{A}_{obsd} - \delta^{A}_{0} = \frac{[D]_0 \cdot K_C^{AD}}{1 + [D]_0 \cdot K_C^{AD}} (\delta^{A}_{AD} - \delta^{A}_{0}) \qquad (3\text{-}8)$$

By rearranging equation (3-8), an analogy of the Benesi-Hildebrand equation expressed in chemical shift is obtained under the condition of $[D]_0 >> [A]_0$:

$$\frac{1}{\delta^{A}_{obsd} - \delta^{A}_{0}} = \frac{1}{K_C^{AD} (\delta^{A}_{AD} - \delta^{A}_{0})} \cdot \frac{1}{[D]_0} + \frac{1}{\delta^{A}_{AD} - \delta^{A}_{0}} \qquad \textbf{(3-9)}$$

where δ^{A}_{0} is the chemical shift of acceptor protons in uncomplexed form, δ^{A}_{obsd} is the observed chemical shift of the acceptor protons in the complexing media, δ^{A}_{AD} is the chemical shift of acceptor protons in the pure complex state. This calculation can be analogously written for chemical shifts of donor, while changing the concentration of acceptor in the system when $[A]_0 >> [D]_0$.

Based on the methods discussed above, complex formation between membrane-resident electron-accepting groups and model electron donating components in liquid mixtures has been studied using the functional compounds described in Chapter 2 including 4-maleimidobenzoyl chloride, 4-phthalimidobenzoyl chloride, 4-tetrachlorophthalimidobenzoyl chloride and 4-succinimidobenzoyl chloride as model electron-accepting components. Styrene and ethylbenzene served as model electron-donating components. Influence of substituents on the imide ring of model electron-accepting compounds on complex formation and differences in complexation strengths of electron-accepting components complexing with various electron-donating compounds have also been evaluated.

Formation constants of maleic anhydride-styrene complexes have been reported to be temperature-dependent [62]. Complexation strength drops 17 times with increasing temperature from 25°C to 33°C. This unique dependence of complexation on temperature provides the possibility to reversibly control the strength of complexation. Mass transport of specific species complexing with functional groups within membranes can be altered by changing temperature in temperature dependent affinity-based membrane separation processes. Temperature dependence of MIBC-aromatic compounds complex formation constant has been investigated using the NMR method.

3.2 Experimental methods

Complexation between maleimide-based model electron-accepting compounds and electron-donating compounds was confirmed by spectrophotometric studies. Complexation constants were evaluated via UV and NMR methods as described below.

3.2.1 Materials

Model electron-accepting compounds used in these studies were synthesized as described previously in Chapter 2. Due to the insolubility of the imidobenzoic acid in most nonpolar solvents, the corresponding acid chlorides were used as model electron-accepting compounds. Styrene and ethylbenzene served as model electron-donating compounds. Styrene was washed with 5% aqueous NaOH, then with water, dried with $MgSO_4$, and distilled under reduced pressure in the presence of an inhibitor. Ethylbenzene (Sigma) was used without further purification. Chloroform was used as solvent in all measurements. Chloroform-d_1 used for NMR measurements was obtained from Aldrich, and contains 0.3% tetramethyl-silane (TMS) as an internal standard.

3.2.2 Comparison of UV spectra of various donor-acceptor systems

A series of UV spectra of maleimidobenzoyl chloride and other model electron accepting compounds in different solvent systems (cyclohexane, ethylbenzene and styrene mixed with chloroform respectively) were measured at 300-420 nm. Concentrations of the model electron-accepting compounds and model electron-donating compounds were carefully controlled to be identical in all measurements. Stock solutions of model electron-accepting compounds in chloroform and cyclohexane, ethylbenzene and styrene solutions in chloroform with identical concentrations were prepared. A 1.0 ml aliquot of the stock solution was added to each of four 5 ml volummetric flasks. Chloroform in the samples was carefully removed by flushing with dry nitrogen gas. After the samples were dried, different electron-donor solutions with the same concentration were added to each sample, respectively. A solution of pure electron-accepting compound in chloroform with the same concentration was measured as well for comparison.

Ultraviolet (UV) absorption spectra were measured with a Hewlett-Packard 8452

diode array spectrophotometer, using 5 mm quartz cuvette at room temperature referenced against chloroform solutions containing the same amount of the respective electron-donating compound. Optical densities were controlled in the range of 0.100 - 0.900 by adjusting concentrations of electron-accepting compounds in each sample.

3.2.3 Complex association constant determined by UV spectra

A series of UV absorption spectra of maleimidobenzoyl chloride (MIBC) solutions with various concentrations of styrene in chloroform were measured at room temperature against reference solutions containing identical concentrations of styrene in complexing solutions. Absorbance of these solutions at 310 nm, 316 nm, 320 nm and 330 nm were measured to obtain the apparent molar absorptivity for calculating the complex association constant at each wavelength. Molar absorptivity of uncomplexed MIBC was also determined at these same wavelengths. MIBC-styrene complexing solutions always contain constant concentrations of MIBC with varying concentrations of styrene. Concentrations of MIBC in all the samples were approximately 0.002 M. Styrene concentrations of samples and references were controlled to be equal (0.5 M$\leq\chi\leq$3.5 M).

Complex formation constant of MIBC-ethylbenzene complexes were evaluated under same conditions using this same protocol.

3.2.4 Evaluation of complex association constants using NMR methods

Identical amounts of MIBC were weighed into each standard NMR tube. Five samples were prepared. Various volumes of styrene were added to each sample. Chloroform-d_1 was then added and the total volume of solvent added into each NMR tube was controlled to be identical. In this way, concentrations

of MIBC in samples were identical, approximately 0.15M. Concentrations of styrene varied from 1.0 M - 2.5 M, which are in large excess to that of MIBC in complexing solutions. MIBC-ethylbenzene complexing solutions were similarly prepared.

Proton nuclear magnetic resonance (NMR) spectra of complexing solutions were obtained on a General Electric QE-300 MHz spectrometer. Tetramethylsilane was used as the internal proton standard. Chemicals shifts of MIBC were monitored and expressed in hertz (Hz). The temperature-dependence of complex association constants was determined using the spectrometer's probe temperature control.

3.3 Results and Discussion

3.3.1 Complexation of various electron donor-acceptor systems

Maleic anhydride/aromatic substance 1:1 complex formation has been confirmed via spectrophotometric studies [53, 54]. In aromatic solvents, ultraviolet absorption spectra of maleic anhydride are greatly intensified, and the onset of a red-shifted absorption progressively increases as alkyl substitutions of the aromatic ring increase. Particularly with styrene, a marked bathochromic shift of the absorption spectra has been observed. This type of shift, however, has not been observed in the absorption spectra of maleic anhydride in various aliphatic solvents.

Complexation between maleimide and aromatic electron-donating compounds has not been so easily proven, and even partial complexation between maleimide and styrene is probably negligible [62]. However, substitution of the amide function on maleimide appears to greatly increase the charge-transfer interaction of N-substituted maleimides with styrene [52].

In order to elucidate whether specific complexation between maleimide-based functional groups coupled to polymers comprising pervaporation membranes and

electron-donating components in mixtures to be separated is strong enough to facilitate the selective permeation of the components through polymer membrane, MIBC and similar compounds were used as model electron-accepting compounds to study complexing ability of N-substituted maleimides with electron-donating components in organic liquid mixtures.

The ultraviolet absorption spectra of MIBC in chloroform containing various solvent components are depicted in Figure 3.1. UV absorption spectra of this N-benzoyl chloride substituted maleimide in various solvents exhibit characteristics similar to that of maleic anhydride complexing solutions. Bathochromic shifts of MIBC absorption in styrene/chloroform and ethylbenzene/chloroform from the absorption of pure MIBC in chloroform are observed. The spectrum in styrene is more red-shifted than that in ethylbenzene. The shoulder portion of the absorption spectra of MIBC in ethylbenzene and styrene (305nm - 370nm) are intensified, most notably in styrene. Unequivocal experimental confirmation of the existence of a unique complex absorption maximum was unfortunately impossible due to the strong absorption of donor components in the solvent and the overlap of the absorption of uncomplexed MIBC in the region of complex absorption.

To prove that the intensification and displacement of the absorption spectra of MIBC in chloroform containing aromatic compounds are due to specific complexation between MIBC and the aromatic compounds in solvent, an absorption spectrum of MIBC in cyclohexane/chloroform having identical concentration as aromatic solutions, chosen to represent MIBC in structurally similar aliphatic solvents, is shown in Figure 3.1 as well. The absorption curve of MIBC in cyclohexane/chloroform has the same shape as that of MIBC in chloroform. A small displacement observed can be regarded as a solvent effect due to dielectric constant differences.

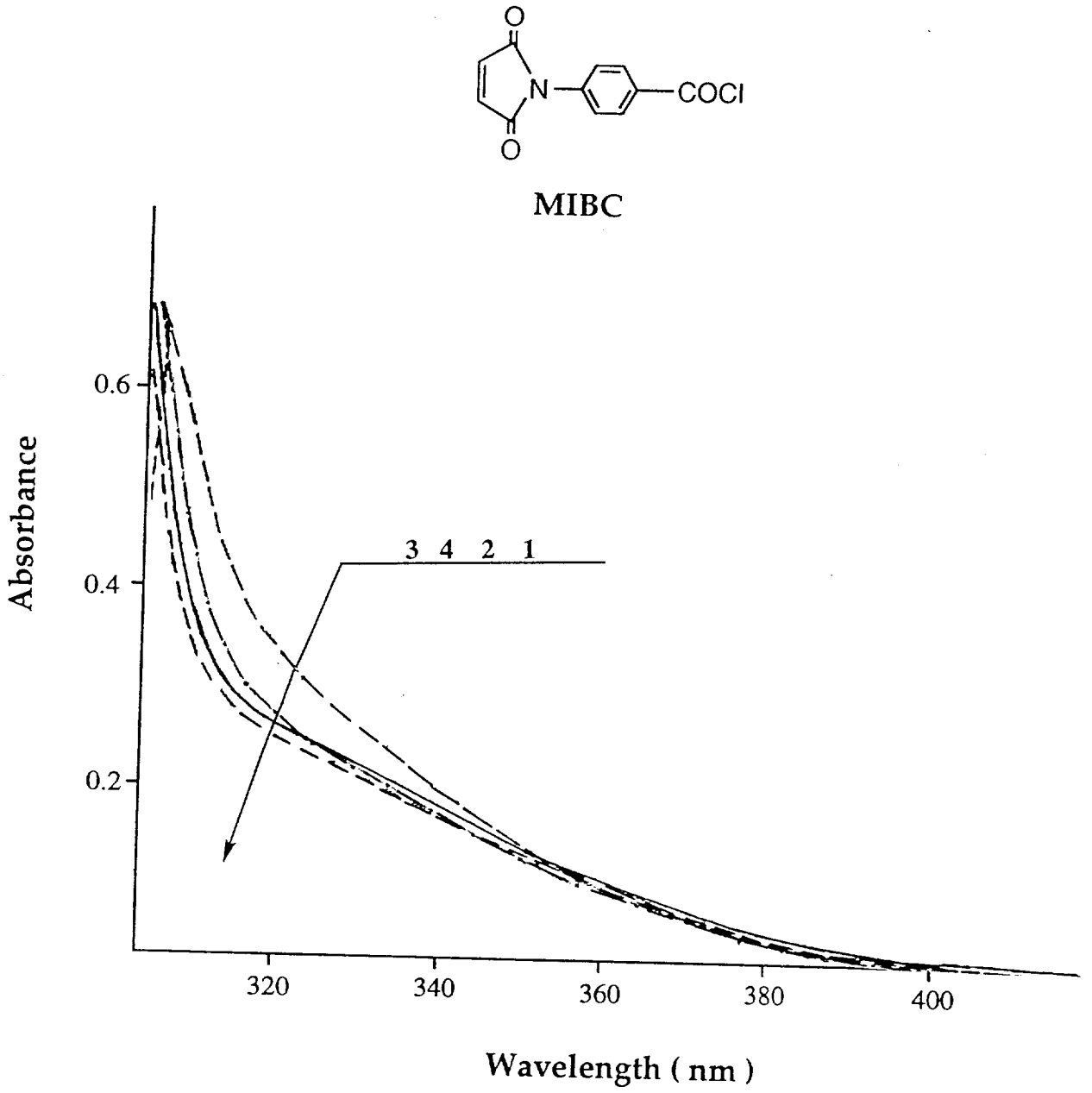

Figure 3.1 UV absorption spectra of MIBC in chloroform with different components: [MIBC] = 8.8 x 10^{-4} M.
(1) Styrene; (2) Ethylbenzene; (3) Cyclohexane; (4) chloroform.

Complexation between MIBC and aromatic compounds was confirmed by bathochromic displacements and intensified shoulders of MIBC absorption spectra in aromatic solvents. These effects are not observed in the case of aliphatic solvents. Going from ethylbenzene to styrene, the displaced and intensified absorptions are further shifted most likely due to the conjugated structure of styrene, which makes it a better electron donor. Therefore, the stabilities of the complexes can be slightly enhanced by the presence of substituents on the aromatic ring of the donor component, which increase the donor electron density.

Absorption spectra of MIBC in chloroform containing various components demonstrate that complex-forming capabilities of MIBC are more significant with styrene than with ethylbenzene (Figure 3.1). This capability was further confirmed by the absorption spectra of MIBC in chloroform containing different concentrations of styrene and ethylbenzene, respectively (Figure 3.2, 3.3). Increasing the concentration of aromatic compound in the solution shifts spectra to longer wavelengths stepwise from lower to higher aromatic concentration. Larger spectral alterations appear for styrene than ethylbenzene with identical variations in concentration.

A complex structure, in which the double bond of maleic anhydride is centrally located above two carbons para to each other across the benzene ring has been proposed for the benzene-maleic anhydride complex [51]. To confirm that this might also be the case for complexes of N-substituted maleimides and aromatic compounds, the absorption spectra of a structurally similar N-substituted aromatic succinimide, 4-succinimidobenzoyl chloride, in chloroform containing various complexing components are compared to that of MIBC. Results are shown in Figure 3.4. No absorption bands analogous to those of MIBC-aromatic compounds complexes are apparent. Only small random shifts, which can be regarded as solvent effects, are observed. *These results clarify the essential role of the double bond of N-substituted maleimides in the*

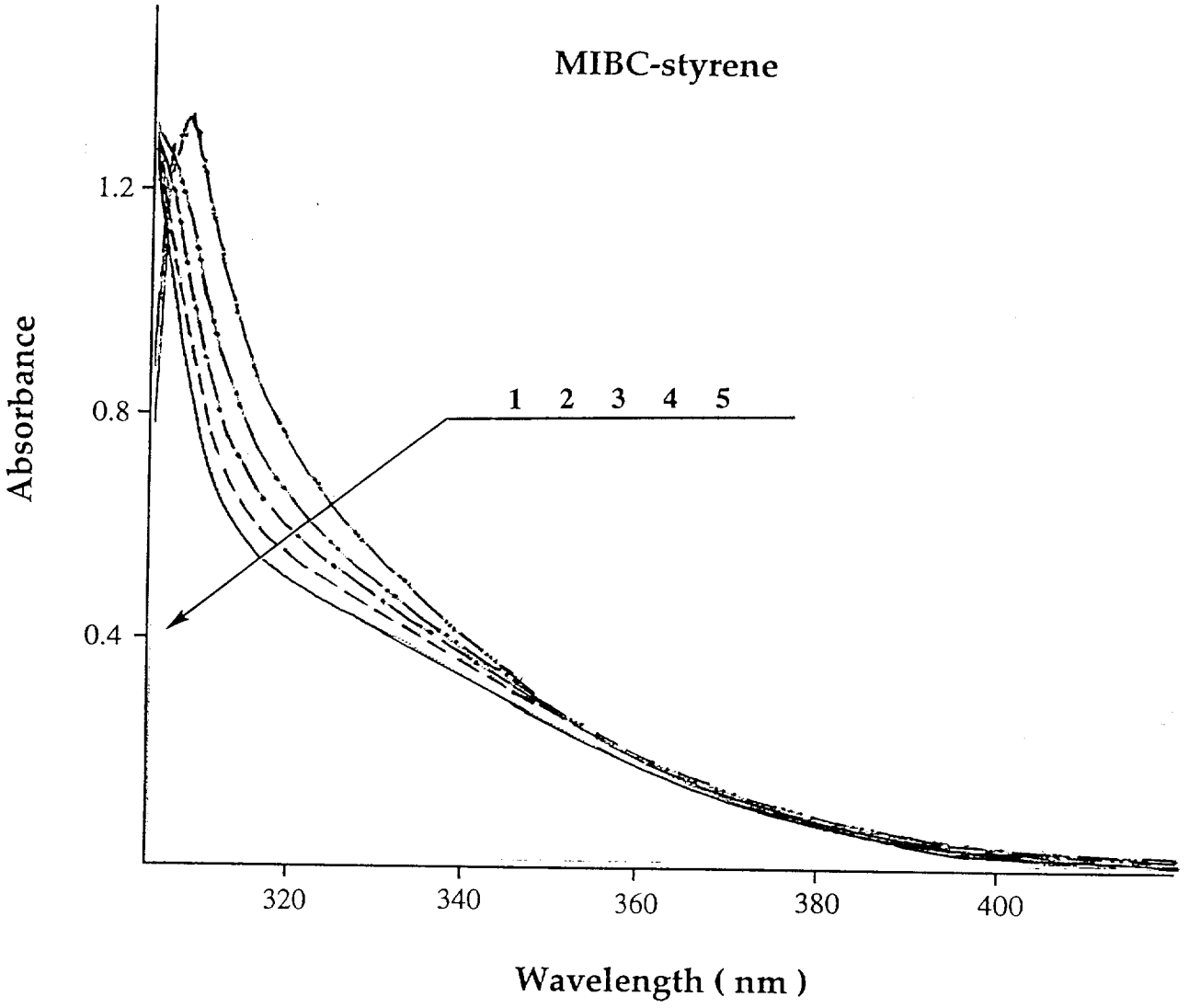

Figure 3.2 Red-shift of absorption bands of complexed MIBC with increasing concentration of styrene in chloroform.
Mole fraction of styrene in chloroform: (1) 0.02, (2) 0.04, (3) 0.10, (4) 0.20, (5) 0.30. [MIBC] = 1.658 x 10^{-3}M

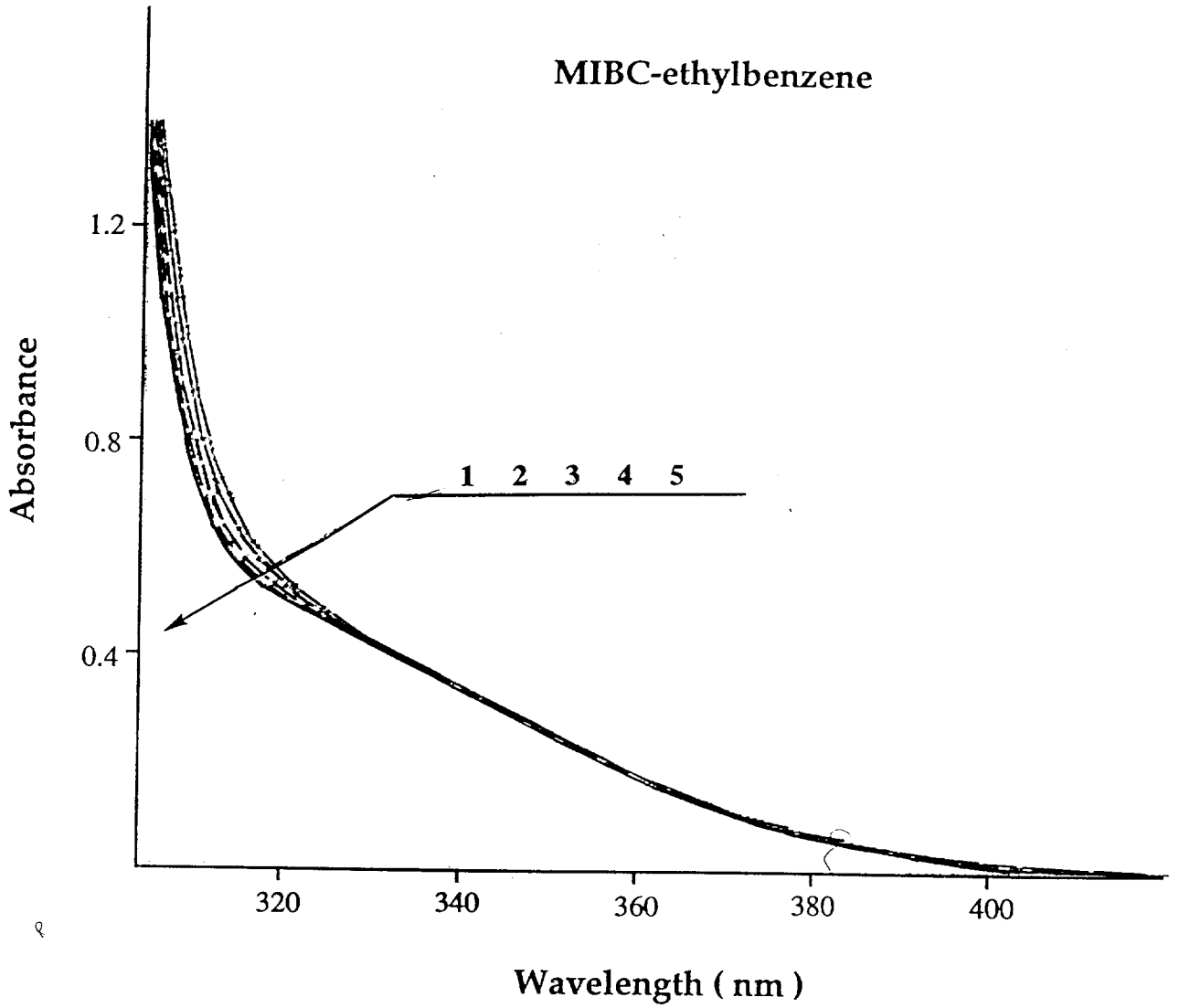

Figure 3.3 Red-shift of absorption bands of complexed MIBC with increasing concentration of ethylbenzene in chloroform.
Mole fraction of ethylbenzene in chloroform: (1) 0.02, (2) 0.04, (3) 0.10, (4) 0.20, (5) 0.30. [MIBC] = 1.658 x 10^{-3}M

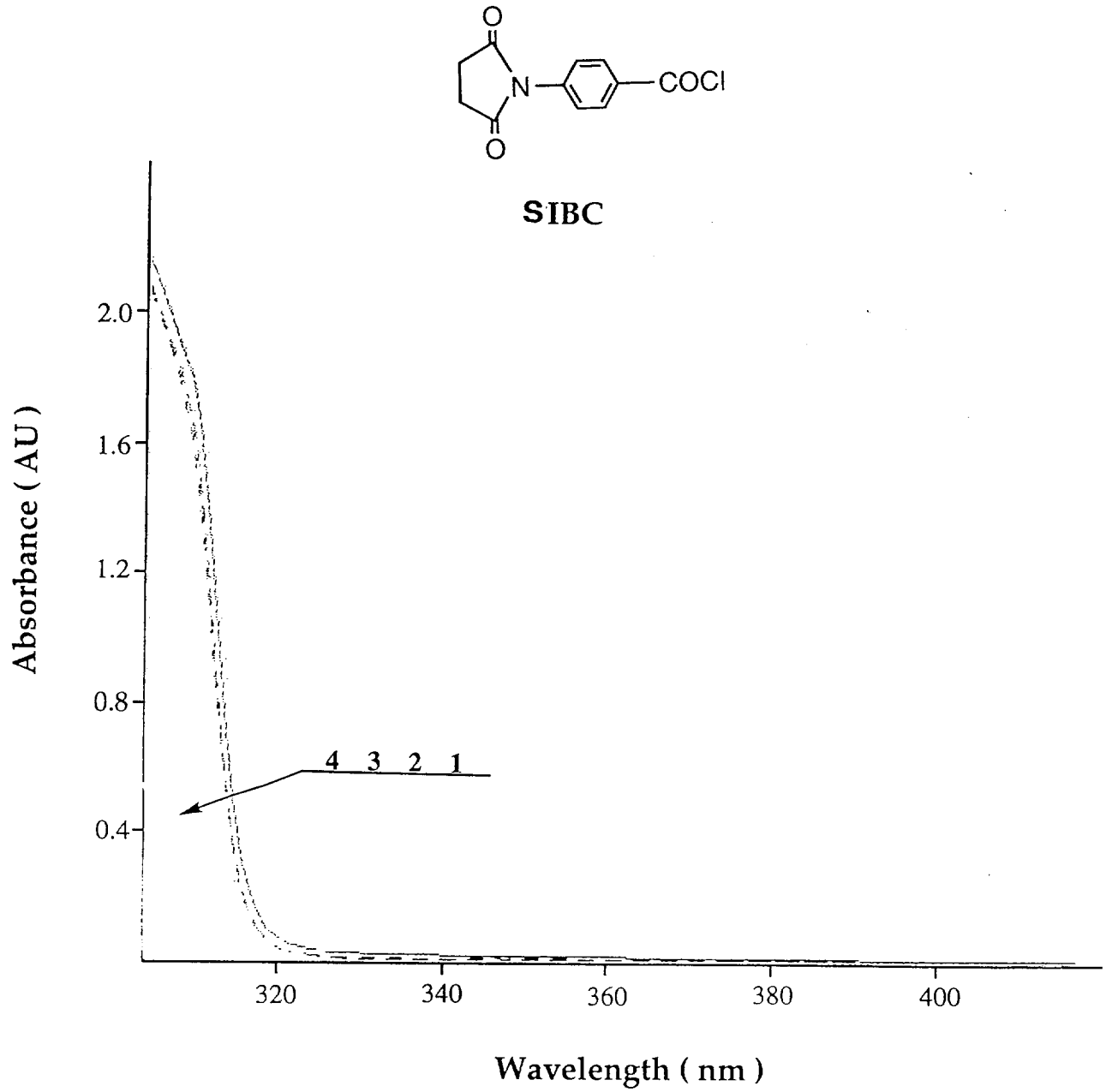

Figure 3.4 UV absorption spectra of SIBC in chloroform with different components: [SIBC] = 9.2×10^{-4} M

(1) Styrene; (2) Ethylbenzene; (3) Cyclohexane; (4) chloroform.

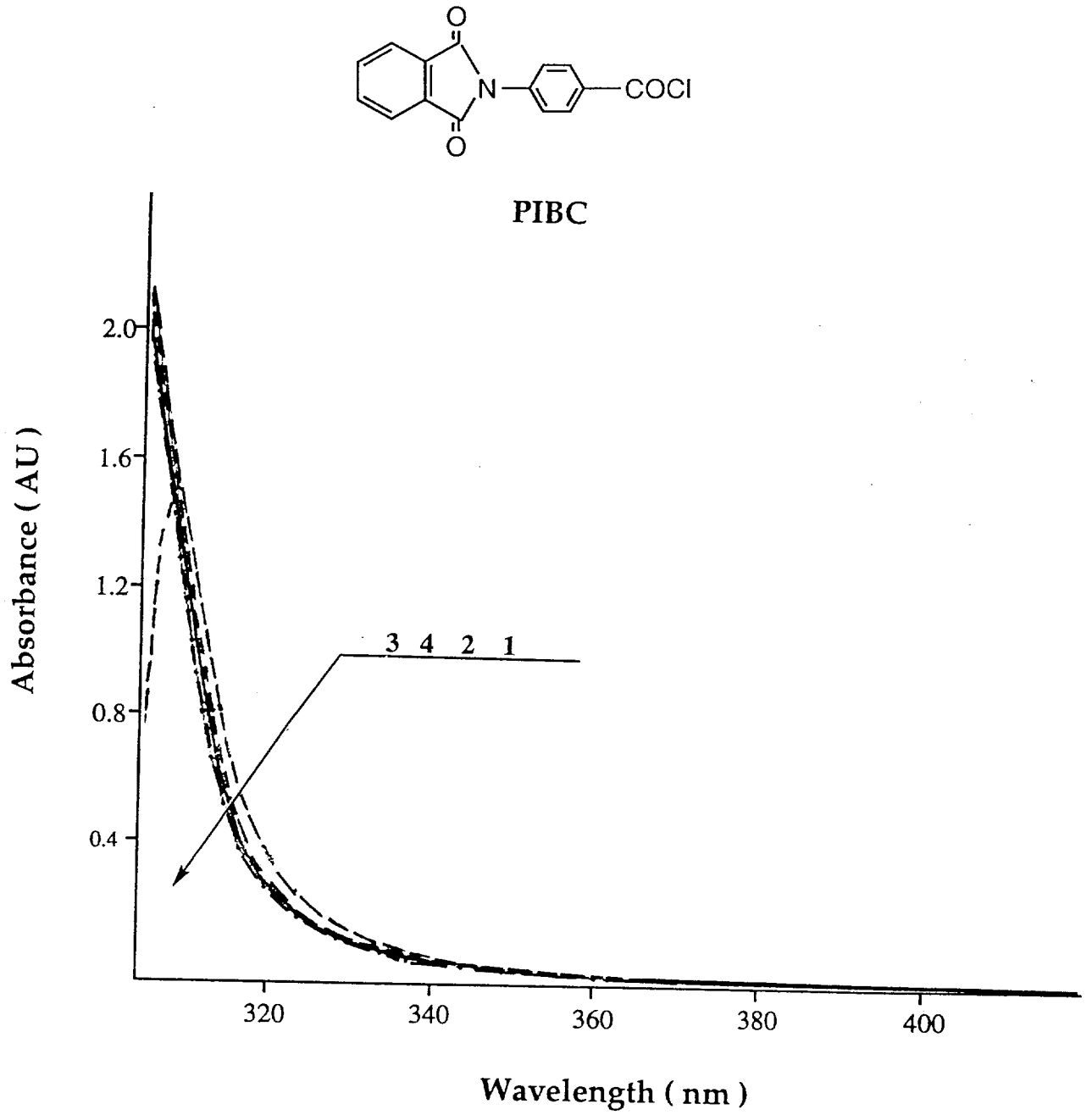

Figure 3.5 UV absorption spectra of PIBC in chloroform with different components: [PIBC] = 8.9×10^{-4} M
(1) Styrene; (2) Ethylbenzene; (3) Cyclohexane; (4) chloroform.

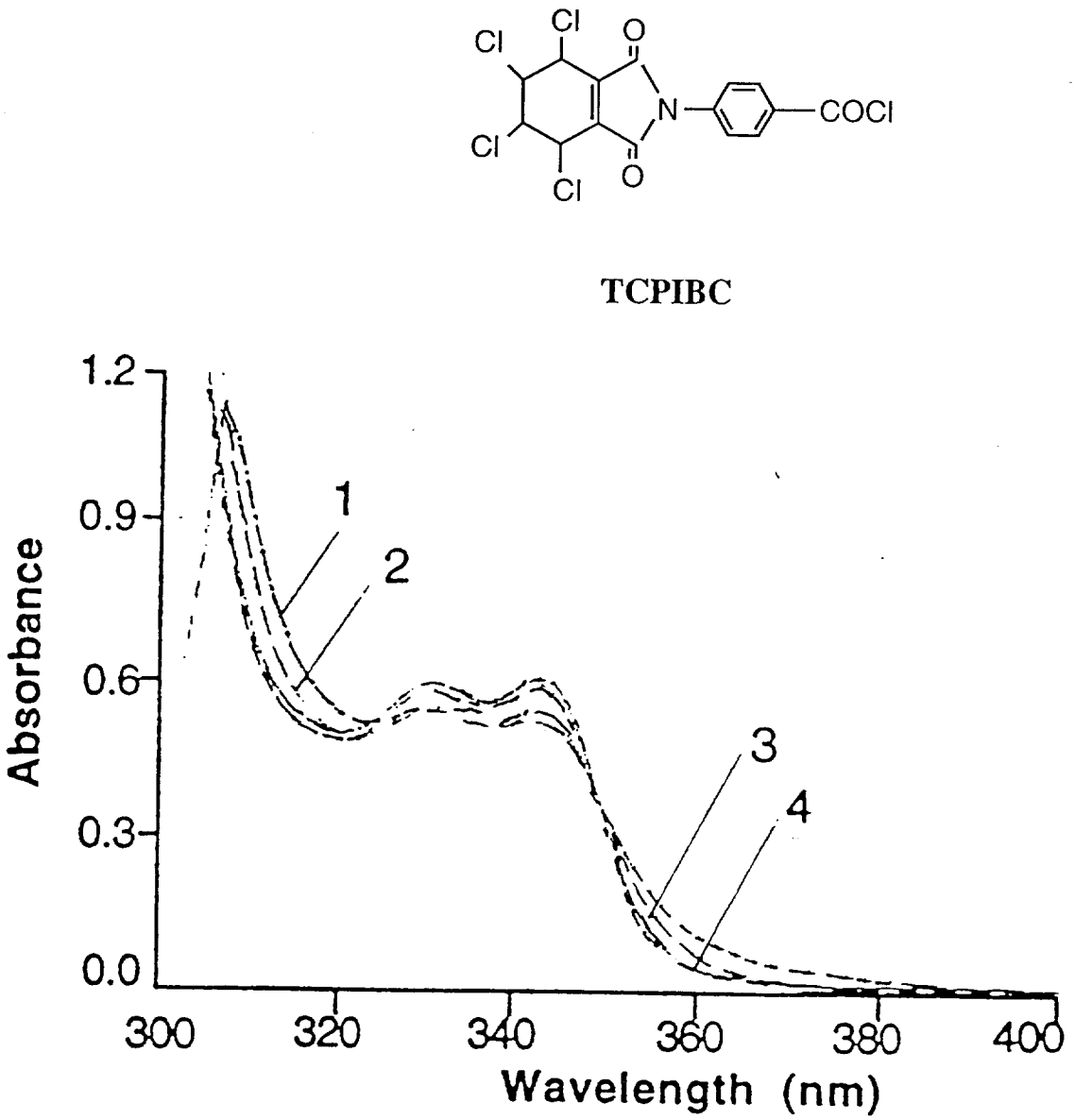

Figure 3.6 UV absorption spectra of TCPIBC in chloroform with different components: [TCPIBC] = 8.9 x 10^{-4} M
(1) Styrene; (2) Ethylbenzene; (3) Cyclohexane; (4) chloroform.

formation of the charge-transfer complexes, and give further evidence for specific complex-forming capabilities of N-substituted maleimides with aromatic electron-donating compounds.

Figure 3.5 and 3.6 show absorption spectra for phthalimidobenzoyl chloride (PIBC) and tetrachlorophthalimidobenzoyl chloride (TCPIBC) in chloroform containing different electron-donating components. Only small red-shifts and intensified absorptions specific to PIBC-aromatic compounds complexes are observed in absorption spectra of PIBC in chloroform containing either styrene or ethylbenzene compared to that in chloroform or cyclohexane/chloroform. Complexation between PIBC and aromatic compounds is greatly reduced because of the benzene ring in the imide structure. This conjugated system makes PIBC a poor electron acceptor as compared to MIBC. Additionally, a large steric hindrance due to the phenyl ring in PIBC makes the imide ring more difficult to coordinate to aromatic compounds to yield electron charge-transfer complexes.

Compared to PIBC, TCPIBC exhibits an increased ability to form electron charge-transfer complexes. Larger bathochromic displacements and greater intensifications of TCPIBC absorptions in chloroform containing either styrene or ethylbenzene are observed relative to that in chloroform alone or chloroform containing cyclohexane. In this case, multiple electron-withdrawing groups on the phenyl ring of TCPIBC provide sufficient electron withdrawing to allow TCPIBC to serve as a better electron acceptor. Compared with MIBC, however, there is no apparent improvement in electron-accepting properties found in TCPIBC. The large steric hindrance of the phenyl group connected to the imide ring appears to hinder TCPIBC-aromatic complexation despite improved electron acceptor properties.

3.3.2 Complexation constants determined via the UV methods

Formation of 1:1 complexes between 4-maleimidobenzoyl chloride (MIBC) and aromatic compounds such as styrene or ethylbenzene was readily confirmed by the previous spectrophotometric studies of MIBC in various solvent systems. The stability of MIBC-aromatic complexes is strongly dependent on the structural and electronic properties of the aromatic electron-donating compounds. In the cases of styrene and ethylbenzene, the conjugated system of styrene makes it a better electron donor, yielding larger spectral displacements and intensifications. To ensure that a more stable complex was formed between MIBC and styrene than MIBC and ethylbenzene, a quantitative evaluation of the association constant of complexation was made, based on the UV data.

Based on the Benesi-Hildebrand method [58], the equilibrium constants for MIBC-styrene and MIBC-ethylbenzene complexing systems were determined by UV spectroscopy. The UV absorption spectra of MIBC-styrene and MIBC-ethylbenzene complexing solutions in chloroform containing different concentrations of styrene or ethylbenzene respectively are shown in Figure 3.2, 3.3. The strong absorption band of the $n \rightarrow \pi^*$ excitation in uncomplexed MIBC occurs at a wavelength close to that of complexed MIBC. In addition due to high concentration of either styrene or ethylbenzene in the complexing solutions and strong absorption of either styrene or ethylbenzene at the shorter wavelength, absolute detection of absorption maximum specific to the complex was difficult. Quantitative evaluation of association constants of MIBC-styrene and MIBC-ethylbenzene was made in the region of the displaced and intensified shoulder of the spectra ranging from 310 - 330 nm. Using the Benesi-Hildebrand equation to evaluate complexation constants, negligible acceptor absorption was assumed. In the case of MIBC-aromatic complexes, large overlap appears due to the absorption of uncomplexed MIBC. The Benesi-Hildebrand equation is no longer

suitable in this case. The equation derived by Ketelaar and coworkers [59], where absorption of the complexing solution is compensated for absorption due to donor components, and absorption due to acceptor components is taken into account, is employed. The expression is given by equation (3-7).

The absorption intensities of each complexing solution and free MIBC solution at several wavelengths are determined from the spectra. The corresponding apparent molar absorptivity of MIBC-styrene and MIBC-ethylbenzene complexing solutions and the molar absorptivity of the uncomplexed MIBC are calculated from the Beer's Law linear relationship, $A=\epsilon cl$, at each wavelength and listed in Table 3.1, 3.2. It can be seen that absorption intensities increase systematically with increasing concentrations of styrene or ethylbenzene in complexing solutions. These data can be interpreted as the occurrence of complex formation. Evaluation of K_C^{AD} and ϵ_λ^{AD} for MIBC-styrene

Table 3.1 The appearent molar absorptivities of MIBC-styrene complexing solutions. ($C_{MIBC} = 1.658 \times 10^{-3}$M)

styrene concentration(M)	ε_{330nm}	ε_{320nm}	ε_{316nm}	ε_{310nm}
0.00	459	545	593	771
0.46	513	623	688	907
1.09	545	680	761	1022
1.89	572	742	846	1161
3.17	642	865	1008	1413

Table 3.2 The appearent molar absorptivities of MIBC-ethylbenzene complexing solution. ($C_{MIBC} = 1.774X10^{-3}M$)

ethylbenzene concentration(M)	ε_{320nm}	ε_{320nm}	ε_{316nm}	ε_{310nm}
0.00	459	545	594	771
0.61	466	561	618	817
1.08	467	571	634	852
1.91	473	591	667	922
2.67	477	606	691	976

complexes was made at certain wavelengths by plotting experimentally determined values of $1/(\epsilon_\lambda^{AD} - \epsilon_\lambda^{A})$ at a given wavelength versus the reciprocal of styrene mole fraction. Linearity, as required for a 1:1 charge-transfer complex, was obtained at each wavelength (Figure 3.7, 3.8). Increasing deviation from linearity at low styrene and ethylbenzene concentration was observed. This deviation is expected because this corresponds to the breakdown of the assumption of $[D]_0 >> [A]_0$ required for formulation of equation (3-7). Values of K_C^{AD} and ϵ_λ^{AD} are calculated from the slopes and intercepts of these lines for each wavelength and are listed in Table 3.3.

Because the intensifications and displacements of the spectra were rather small in the case of MIBC-ethylbenzene complexing solution, experimental error has a great influence on the measurement. In some cases, the experimental error can be larger than the intensification of the spectrum, thus making a quantitative measurement of intensified absorbance difficult. All absorption values were corrected by the absorbance at a specific wavelength (500nm) where it can be considered that no absorption of

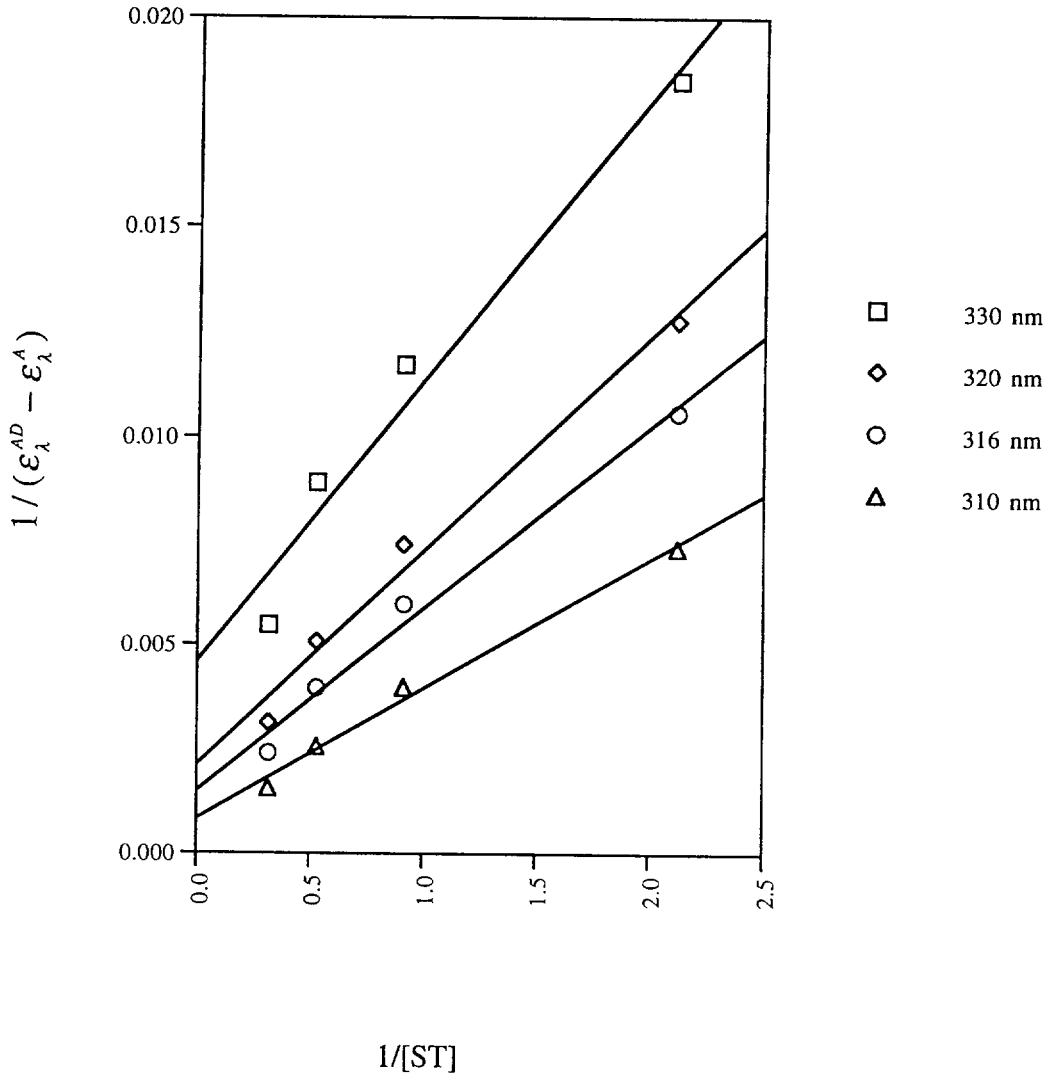

Figure 3.7 Evaluation of K_C^{AD} for the MIBC-styrene complex at 310, 316, 320 and 330 nm.

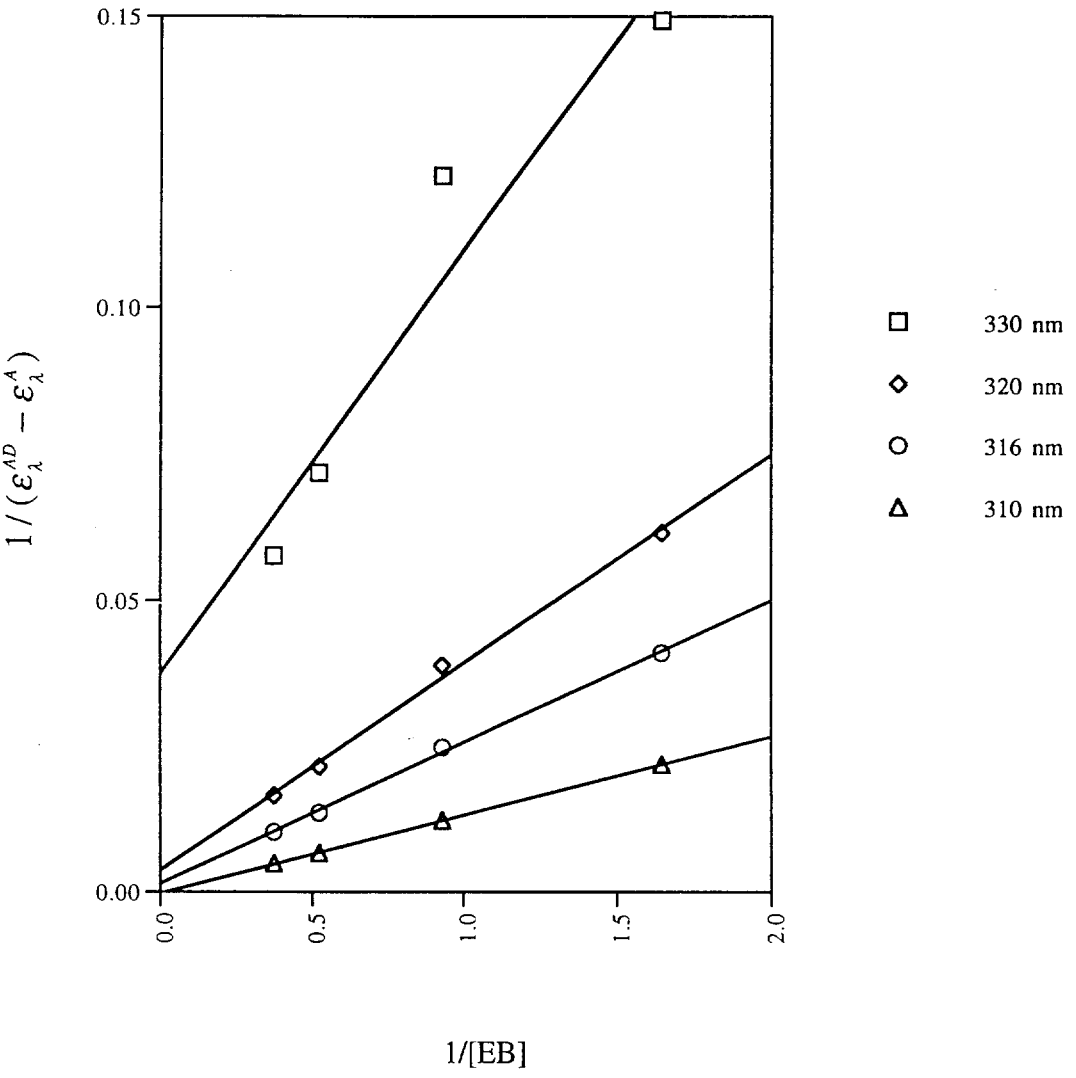

Figure 3.8 Evaluation of K_C^{AD} for the MIBC-ethylbenzene complex at 310,316, 320 and 330 nm.

Table 3.3 Association constants for MIBC-styrene and MIBC-ethylbenzene complexes formation (M^{-1})

	MIBC-styrene		MIBC-ethylbenzene	
λ(nm)	K_C^{AD}	ϵ_C^{AD}	K_C^{AD}	ϵ_C^{AD}
330	0.68	676	0.52	4876
320	0.42	1016	0.11	811
316	0.34	1262	0.06	1323
310	0.27	---	0.02	---

any species in the complexing solution appears. This procedure gave highly reproducible absorbance values and reasonable intensity increases. However, the calculated K_C^{AD} and ϵ_λ^{AD} values are very sensitive to experimental error. ϵ_λ^{AD} values are obtained from intercepts of the plotted straight lines with the ordinate in Benesi-Hildebrand plots, which are close to the origin. Small experimental errors can lead to a negative intercept which is not in agreement with the experimental data. K_C^{AD} values are determined from both the slopes and the intercepts. Inaccurate data will have even larger influence on accuracy of K_C^{AD}. It must be re-emphasized that, due to the overlap of the absorption of both donor and acceptor components with the charge-transfer band in MIBC-aromatic substances complexing systems, the calculation is inaccurate.

Calculated complexation constants K_C^{AD} are found to be wavelength dependent in both MIBC-styrene and MIBC-ethylbenzene complexing systems. This wavelength-dependence for calculated complexation constants K_C^{AD} has been observed in many systems when the experimental condition $[A]_0 << [D]_0$ is used [63]. This implies that

complexes of other stoichiometries are formed in addition to 1:1 complexes in MIBC-styrene and MIBC-ethylbenzene complexing systems even though the principal species formed are 1:1 complexes [64]. It has been reported that the linearity of Benesi-Hildebrand plots is not a sufficient criterion for the presence of only 1:1 complexes. In systems where the 1:1 complex is the primary species coexisting with complexes of other stoichiometries, linearity of Benesi-Hildebrand plot can still be obtained, but K_C^{AD} becomes dependent on the wavelength. Also this wavelength-dependence is not observed in complexing systems with equimolar mixtures of donors and acceptors. In complexation studies of MIBC-styrene and MIBC-ethylbenzene systems, it is not practical to use equimolar mixtures of MIBC and styrene (or ethylbenzene). Concentrations of either styrene or ethylbenzene are in large excess to that of MIBC, which favors multimolecular complex formation. Another reason for the variation of calculated K_C^{AD} at different wavelengths is the contribution to the total measured absorption from species other than either MIBC-styrene or MIBC-ethylbenzene complexes, such as complexes formed between MIBC and solvents which compete with donor components in the complexing solutions.

Due to the shortcomings of this method as discussed above, the association constants and molar absorptivities of the complexes could not be determined with any real accuracy. However, the K_C^{AD} values determined in this study are comparable. Comparing the K_C^{AD} values listed in Table 3.3 at each wavelength, association constants for MIBC-styrene complexes are noticeably larger than those for MIBC-ethylbenzene complexes. *More stable complex formation is obtained between MIBC and styrene than MIBC and ethylbenzene.*

3.3.3 Complexation Studies Utilizing the NMR Methods

To overcome the shortages of the spectrophotometric method in MIBC-aromatic compounds complexation studies and to investigate temperature influence on MIBC-aromatic complex formation, an NMR method developed by Hanna and Ashbaugh [60] was employed by monitoring the variation of the chemical shifts of MIBC in MIBC-aromatic complexing solution relative to those of uncomplexed MIBC. One advantage of the NMR method is that measuring a chemical shift peak position is experimentally easier than an intensified absorption intensity. Another benefit is that a relatively larger concentration of each component can be used, which assists complex formation determination.

Chemical shifts of MIBC in solutions with constant MIBC concentration and varying styrene or ethylbenzene concentrations are listed in Table 3.4, 3.5, respectively. For comparison, chemical shifts of uncomplexed MIBC (MIBC in pure d-chloroform) and MIBC in solutions containing cyclohexane representing an aliphatic structurally analogous system are listed in Table 3.6. It is apparent that MIBC readily forms complexes with both styrene and ethylbenzene. The chemical shifts of MIBC display a significant upfield shift in both MIBC-styrene and MIBC-ethylbenzene complexing solutions relative to that of uncomplexed MIBC. This variation of MIBC proton chemical shifts can be ascribed to increasing shielding of MIBC protons due to charge-transfer from either styrene or ethylbenzene. Further evidence for complex formation between MIBC and aromatic substances is given by the donor concentration-dependence of MIBC chemical shift variation in aromatic systems. With increasing concentrations of the aromatic component in the complexing solution, the chemical shifts of MIBC shift further upfield. In contrast, the chemical shifts of MIBC in aliphatic systems such as cyclohexane/chloroform-d_1 are constant even though they shift 10Hz upfield compared to that of uncomplexed MIBC. This variation can be

Table 3.4 Chemical shifts of MIBC in MIBC-styrene complexing solutions (C_{MIBC} = 0.116M, 25°C).

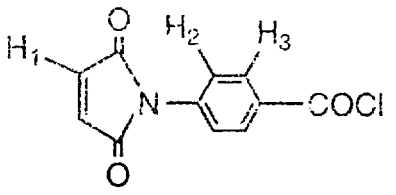

styrene concentration(M)	H_1(Hz)	H_2(Hz)	H_3(Hz)
0.00	2082.49	2295.08	2467.13
1.01	2018.04	2269.34	2444.27
1.34	2000.83	2262.63	2438.06
1.68	1986.90	2251.50	2428.50
2.01	1972.56	2247.01	2426.76

Table 3.5 Chemical shifts of MIBC in MIBC-ethylbenzene complexing solutions (C_{MIBC} = 0.116M, 25°C).

ethylbenzene concentration(M)	H_1(Hz)	H_2(Hz)	H_3(Hz)
0.00	2082.49	2295.08	2467.13
0.98	2027.63	2274.63	2448.68
1.31	2010.36	2269.09	2443.58
1.65	1994.33	2264.07	2438.01
1.97	1986.07	2259.00	2433.58

Table 3.6 Chemical shifts of MIBC in cyclohexane/chloroform-d_1 solutions (C_{MIBC} = 0.116M, 25°C).

cyclohexane concentration(M)	H_1(Hz)	H_2(Hz)	H_3(Hz)
0.00	2082.49	2295.08	2467.13
1.74	2074.45	2296.11	2465.18
3.52	2074.12	2297.48	2466.82

considered as a solvent effect due to alteration of dielectric constant of the system. From the listed data, it also can be seen that chemical shifts of protons on the imide ring shift upfield further than those of the MIBC phenyl ring compared to corresponding positions for uncomplexed MIBC in both styrene and ethylbenzene complexing solutions. These results further confirm the earlier evidence that both MIBC-styrene and MIBC-ethylbenzene complex formation are the result of MIBC imide ring coordination with aromatic rings of either styrene or ethylbenzene. The olefinic imide ring protons lie in the shielding region of the aromatic ring, which provides a larger upfield shift to these protons over the protons on the phenyl rings. The influence of the aromatic ring on the MIBC phenyl ring is smaller because the phenyl ring is distanced from the aromatic ring of the donors.

Table 3.7, 3.8 list variations in MIBC proton chemical shifts detected in MIBC-styrene and MIBC-ethylbenzene complexing solutions relative to uncomplexed MIBC chemical shifts. Comparing the variation of chemical shifts of MIBC with styrene to that with ethylbenzene, further upfield shifts are observed for MIBC-styrene with the same alteration of concentration of the aromatic component in the complexing solution than for MIBC-ethylbenzene. Typical plots for the reciprocal of the chemical shift

Table 3.7 Chemical shift variations of MIBC in MIBC-styrene complexing solutions (C_{MIBC} = 0.116M, 25°C).

styrene concentration(M)	ΔH_1(Hz)	ΔH_2(Hz)	ΔH_3(Hz)
1.01	64.45	25.74	22.86
1.34	81.66	32.45	29.07
1.68	95.59	43.58	38.63
2.01	109.93	48.07	40.37

Table 3.8 Chemical shift variations of MIBC in MIBC-ethylbenzene complexing solutions (C_{MIBC} = 0.116M, 25°C).

ethylbenzene mole fraction	ΔH_1(Hz)	ΔH_2(Hz)	ΔH_3(Hz)
0.98	54.86	20.45	18.45
1.31	72.13	25.99	23.55
1.65	88.16	31.01	29.12
1.97	96.42	36.08	33.55

variation of specific protons on MIBC in complexing solutions relative to that in pure d-chloroform ($1/(\delta^A_{obsd} - \delta^A_0)$) against the reciprocal of the mole fraction of styrene and ethylbenzene are shown in Figures 3.9 and 3.10 . Straight lines are obtained in each case. The intercept with the ordinate yields ($\delta^A_{obsd} - \delta^A_0$) and from the slope the product $K_C^{AD}(\delta^A_{obsd} - \delta^A_0)$ is obtained. Thus, association constants for MIBC-styrene and MIBC-

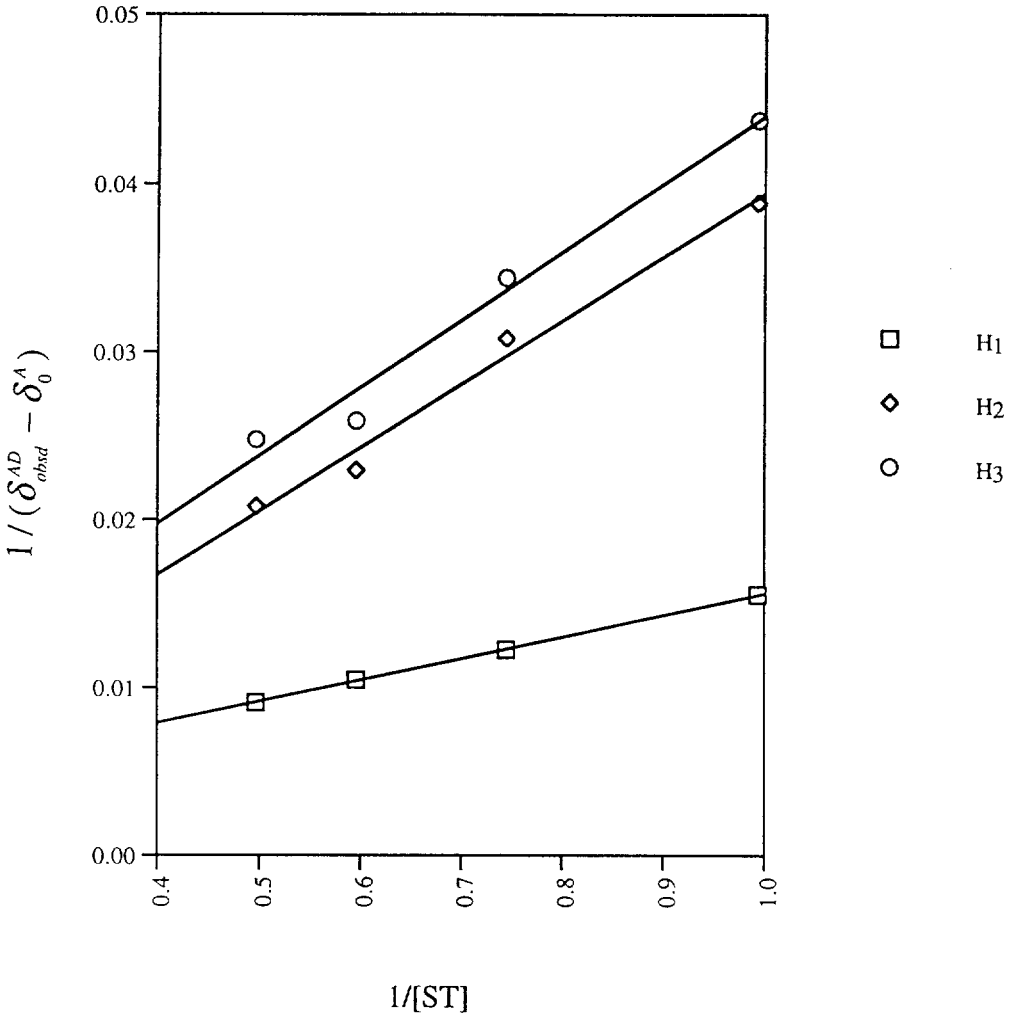

Figure 3.9 Evaluation of K_C^{AD} for the MIBC-styrene complex according to the NMR chemicals shifts of H_1, H_2, H_3.

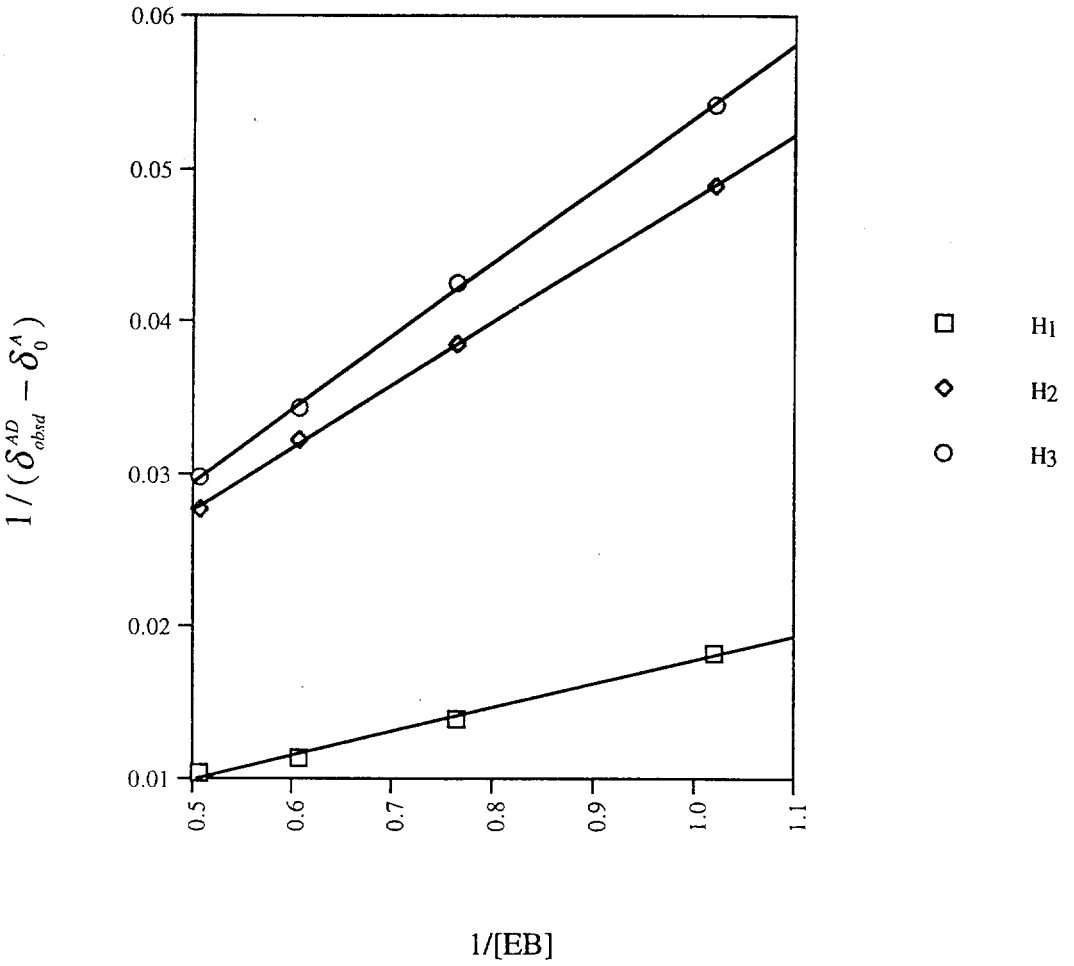

Figure 3.10 Evaluation of K_C^{AD} for the MIBC-ethylbenzene complex according to the NMR chemicals shifts of H_1, H_2, H_3.

ethylbenzene complexes are readily evaluated from the plots and are listed in Table 3.9. Association constants for MIBC-styrene complexes are 1.5 times larger than those for MIBC-ethylbenzene complexes. Compared to association constants evaluated from the chemical shift variation for MIBC imide ring protons, the association constants evaluated from chemical shift variation for MIBC phenyl ring protons are relatively smaller. These results provide a quantitative evidence that MIBC-aromatic complexes formation is due to specific coordination of donor aromatic rings and MIBC imide rings. Additional substituents on both of the rings can dramatically change complexation strengths.

Table 3.9 Assocation constants of MIBC-styrene and MIBC-ethylbenzene complexes (M^{-1}).

	MIBC-styrene	MIBC-ethylbenzene
H_1	0.21	0.13
H_2	0.04	0.04
H_3	0.09	0.11

Temperature dependence of maleic anhydride-styrene complexation strength has been reported. If functional groups coupled to membrane polymer backbones also maintain this property, permeate transport across pervaporation polymer membranes can be adjusted by temperature. Formation constants for MIBC-styrene and MIBC-ethylbenzene complexes were evaluated using the NMR method at 35°C in addition to 25°C. The experimental data and calculated association constants at 35°C are listed in Table 3.10, 3.11 and 3.12. Compared to the corresponding association constants at 25°C, association constants of these complexes are relatively lower at 35°C. The

Table 3.10 Chemical Shifts of MIBC in MIBC-styrene complexing solutions (C_{MIBC} = 0.116M, 35°C)

styrene concentration(M)	H_1	H_2	H_3
0.00	2077.38	2295.53	2465.08
1.01	2025.25	2274.69	2446.11
1.34	2012.17	2269.54	2441.52
1.68	1996.51	2263.37	2435.70
2.01	1983.33	2258.62	2431.33
2.35	1966.6	2251.61	2424.63

Table 3.11 Chemical shifts of MIBC in MIBC-ethylbenzene complexing solutions (C_{MIBC} = 0.116M, 35°C)

ethylbenzene mole fraction	H_1	H_2	H_3
0.00	2077.38	2295.53	2465.08
0.94	2033.78	2280.88	2451.65
1.26	2023.99	2277.50	2448.45
1.57	2004.85	2270.26	2441.53
1.89	1990.54	2265.63	2437.07
2.20	1976.90	2260.49	2431.93

Table 3.12 Association constants of MIBC-styrene and MIBC-ethylbenzene complex formation (M^{-1}, 35°C).

	MIBC-styrene	MIBC-ethylbenzene
H_1	0.10	0.03
H_2	0.11	0.03
H_3	0.10	0.05

interesting point is that the association constants for the MIBC-ethylbenzene complexes drop more rapidly than those for MIBC-styrene complex. At 35°C, association constants for MIBC-styrene complexes are almost 3 times larger than those for MIBC-ethylbenzene complexes. In this case, association constants of MIBC-ethylbenzene drop to 1/5 of the original value while those for MIBC-styrene drop to half of these values with increasing temperature from 25°C to 35°C. Increasing temperature increases the relative differences in complexation strengths. Therefore, selective transport of styrene from styrene/ ethylbenzene mixtures through MIBC-resident membranes should be achieved by increasing temperature even though complexation between MIBC and styrene drops to half strength.

The NMR method used to evaluate complex association constants also has several disadvantages. As with the UV method, plotting $1/(\delta^{A}_{obsd} - \delta^{A}_{0})$ vs $1/[D]_0$ also leads to intercepts close to the origin. The calculated K_c^{AD} is very sensitive to experimental error. Also, NMR is extremely sensitive to small changes in the electronic environment of a magnetic nucleus. It can be an advantage to using NMR to measure chemical shift variations in complexing solutions because weak interactions between electron-donating and electron-accepting components only cause small alterations of

electron environments. But this also can be a disadvantage as chemical shift variations due to other reasons can cause large deviations in the calculated K_C^{AD} from the true values. It has also been reported that chemical shift variations of maleic anhydride and N-substituted imides in aromatic solvents is due to both the larger electron affinity and the polarization of the carbonyl group. In this case, the association constants evaluated from the NMR method will deviate from the true value because the chemical shift variations measured are not only caused by charge-transfer complexation.

Determination of association constants has been made on complexes of MIBC-styrene and MIBC-ethylbenzene. Although none of the methods currently used yields absolute values with high confidence, the comparison of these results suggests that more stable complex can be formed between MIBC and styrene than MIBC and ethylbenzene. MIBC also shows a small temperature dependence while complexing with aromatic compounds.

3.3.4 Future Experiments

Complex formation between N-substituted maleimides and aromatic compounds has been confirmed via spectrometric studies of MIBC-based compounds and SIBC in aromatic and aliphatic solvent systems. Evaluation of complexation constants of MIBC and styrene/ethylbenzene using UV and NMR methods shows that styrene forms a more stable complex with MIBC than ethylbenzene. Absorption spectra of PIBC and TCPIBC, whose structures were designed to adjust the election-accepting properties of these ligands, show the influence of different functional groups attached to the double bond in the imide structure. It can be seen that functional groups attached to the double bond in the imide structure not only changed electron properties of these electron-accepting compounds, but also affected the coordination between electron-donating and electron-accepting compounds. Increasing complexation between N-substituted

maleimides and styrene due to electron-withdrawing N-substitutents is evidenced [52]. Electron-accepting properties are expected to be adjusted by modifying the maleimide with N-substitutents of different electron-donating and withdrawing properties. In this case, the electronic properties of the functional groups are changed without altering the coordination between the electron donor aromatic ring and the double bond in the electron accepting maleimide structure. New maleimide-based compounds with various N-substitutents need to be synthesized and complexation between these new compounds and different aromatic compounds will be investigated. Complexation strength and differences in complexation strength of MIBC complexing with styrene and ethylbenzene give evidence for stronger complexation of MIBC towards styrene. This could facilitate separation of styrene from styrene/ethylbenzene mixtures using a dense polymer membrane coupled with MIBC complexing groups. In this case, competitive complexation of MIBC towards styrene and ethylbenzene in styrene/ethylbenzene mixtures will also be valuable to study.

Chapter 4

Derivatization of Poly(vinyl alcohol) with Maleimide Complexing Agents for Fabricating Pervaporation Membranes

4.1 Introduction

Pervaporation could eventually be regarded as an innovative, energy-saving separation technology. Membranes used in pervaporation are the primary factor determining separation efficiency. The rationale for fabricating improved membranes is based on two factors: the nature of the constituents in the mixtures to be separated, and the degree of separation required. For separation of styrene/ethylbenzene and aromatic/aliphatic mixtures, synthetic polymer membranes bearing functional groups which interact or recognize specific substrates were designed. Functional units showing high affinity toward specific permeants incorporated into a relatively impermeable polymer membrane could enhance both transport selectivity and flux. Complexation between maleimidobenzoyl chloride (MIBC) and aromatic compounds has been discussed extensively in Chapter 3. Specific and selective separation of styrene from styrene/ethylbenzene mixtures and aromatic compounds from aromatic/aliphatic mixtures with derivatized membrane may be realized by incorporating MIBC into dense polymer membranes. Differences in complexation strengths between various aromatic compounds may lead to selective membrane separations.

To optimize separation efficiency, main chain polymers with a high potential for facile modification through well-known synthetic chemistry routes, and demonstrating

acceptable membrane-forming properties and good solvent resistant characteristics (especially in the organic mixtures to be separated) need to be developed for the membrane. Additionally, distributions and densities of affinity functionalities along the polymer main-chains in the membrane need to be adjusted.

According to the criteria for choosing membrane polymer materials, partially hydrolyzed poly(vinyl alcohol) (PVA) was chosen to be coupled with the maleimide-based functional groups. PVA is known to form membranes of good mechanical properties and to have high gas impermeability. Thus, modification of PVA with MIBC is expected to provide membrane materials with high permselectivity and high mechanical stability.

The chemistry of PVA generally utilizes esterification. Conversion of PVA to its acetate is commonplace and can be carried out quantitatively through the reactions of acetic acid, acetic anhydride, or acetyl chloride. Therefore, coupling of maleimide-based complexing compounds to PVA backbone has been attempted by reacting PVA with p-maleimide substituted benzoyl chloride. Succinimidobenzoyl chloride (SIBC) will also be coupled to PVA backbone for comparison. Also, reactions of p-imide substituted benzoyl chloride with isopropanol and PVA with benzoyl chloride were also carried out as model reactions for coupling of PVA with various p-imide substituted benzoyl chlorides.

4.2 Experimental methods

4.2.1 Reagents and solvents

Most reagents and solvents were obtained from Aldrich Co. DMAc was purified using the procedure discussed in Chapter 2. Partially hydrated poly(vinyl alcohol) was a commercially available product with 87-89% hydrolysis of polyvinyl acetate and

molecular weight of 124,000. This polymer was dissolved into DMAc, mixed with benzene, and refluxed with a Dean-Stark apparatus for hours to remove moisture remaining in PVA. Benzene in the PVA-DMAc solution was removed by distillation. Purified PVA-DMAc solutions were kept in a desiccator for further reactions. Benzoyl chloride and isopropanol was used without further purification. Pyridine was dried by refluxing with solid CaO, followed by fractional distillation.

4.2.2 Model reactions

4.2.2.1 Isopropyl maleimidobenzoate

0.5 g of malimidobenzoyl chloride (2.1 mmol) was dissolved into 10 ml chloroform, then 5 ml of isopropanol was added into the MIBC-chloroform solution. The reaction solution was heated to 45°C and stirred overnight. After cooling to room temperature, chloroform and excess isopropanol were removed by rotoevaporation. White powder remaining in the reaction flask was purified by recrystallization using isopropanol. White crystals were obtained with mp 78-80°C. Yield: 67%.
^{1}H-NMR (chloroform-d_1) δ 6.8 (s, 2H), 7.4(m, 2H), 8.2(m, 2H), 1.4(s, 6H), 5.2-5.3(m, 1H).

4.2.2.2 Isopropyl succinimidobenzoate

Using the same synthesis and purification procedure described in section 4.2.2.1, isopropyl succinimidobenzoate was obtained with mp 124-126°C.
^{1}H-NMR (chloroform-d_1) δ 2.9 (m, 4H), 7.4(m, 2H), 8.2(m, 2H), 1.4(s, 6H), 5.5 (m, 1H).

4.2.2.3 Modification of PVA with benzoyl chloride.

1 ml of benzoyl chloride (8.7 mmol) was added to 30 ml of purified PVA-DMAc stock solution (0.3 g PVA). The reaction solution was stirred at room temperature for 48 hours. Then the solution was carefully dropped into distilled water forming a white polymer precipitate in water. The polymer was filtered and dried in a vacuum desiccator.

4.2.3 Modification of PVA with MIBC

4.2.3.1 Derivatization in pyridine

1 g of maleimidobenzoyl chloride (4.2 mmol) was dissolved into 10 ml purified pyridine and added to 30 ml of purified PVA-DMAc solution (0.3 g PVA). The reaction solution was stirred at room temperature. After standing for 24 hours, the solution turned brown. The longer the reaction continued, the darker the solution obtained. Dropping the reaction solution into distilled water, no polymer was precipitated in water.

4.2.3.2 Direct reaction in DMAc

1 g of maleimidobenzoyl chloride (4.2 mmol) was dissolved into 10 ml purified DMAc and added to 30 ml of purified PVA-DMAc solution (0.3 g PVA). The reaction solution was stirred at room temperature. After standing for 48 hours, the solution was carefully dropped into distilled water. A white polymer precipitates in water. This polymer was filtered out and dried in a vacuum desiccator.

4.3 Results and Discussion

New PVA side chain polymers were attempted by reaction of poly(vinyl alcohol)

(PVA) with benzoyl chloride containing maleimide substitutents. The synthetic route is shown in Scheme 4.1.

Conversion of PVA to its acetate can usually be carried out quantitatively by reacting PVA with acetyl chloride. But when the acid group becomes bulky, a quantitative conversion to the ester is not possible. When the molecular weight of PVA is above about 20,000, the degree of esterification is even more restricted. Pyridine is a typical medium used for these esterifications.

Esterification of PVA by MIBC was first carried out by reacting purified PVA-DMAc solution with MIBC in pyridine. At first a light brown solution was formed and after letting the reaction standing overnight, a dark brown solution was formed and no polymer was obtained.

Not knowing the reason for formation of the dark solution, model reactions of MIBC with isopropanol or, alternatively PVA reacting with benzoyl chloride were carried out both with and without pyridine. White polymer product can always be obtained from reacting PVA with benzoyl chloride with and without pyridine. Without pyridine, isopropyl maleiminidobenzoate was obtained by heating MIBC in isopropanol. However, with addition of pyridine in this reaction, a light brown solution forms immediately. After standing the reaction overnight, the solution becomes even darker. From these results, it can be seen that pyridine reacts with MIBC, although the exact reaction mechanism or product is not clear.

Esterification of PVA by MIBC was also carried out by reacting purified PVA with MIBC at different temperatures and with different ratios of starting materials. At high temperatures, a polymer gel is usually obtained. At room temperature, an off-white polymer is obtained by precipitation in water. Nevertheless, after drying the polymer in a vacuum desiccator, the polymer forms a gel in DMAc. From these results, it can seen that even though a white linear polymer is obtained from reacting PVA with MIBC

directly, a crosslinked polymer usually forms after polymer is separated from the polymer solution. Also, crosslinking does not happen in other polymer products obtained by reacting PVA with other benzoyl chloride containing imide moiety substituents. Therefore, although the reason for polymer crosslinking is not certain, MIBC groups appear highly reactive and affect this result.

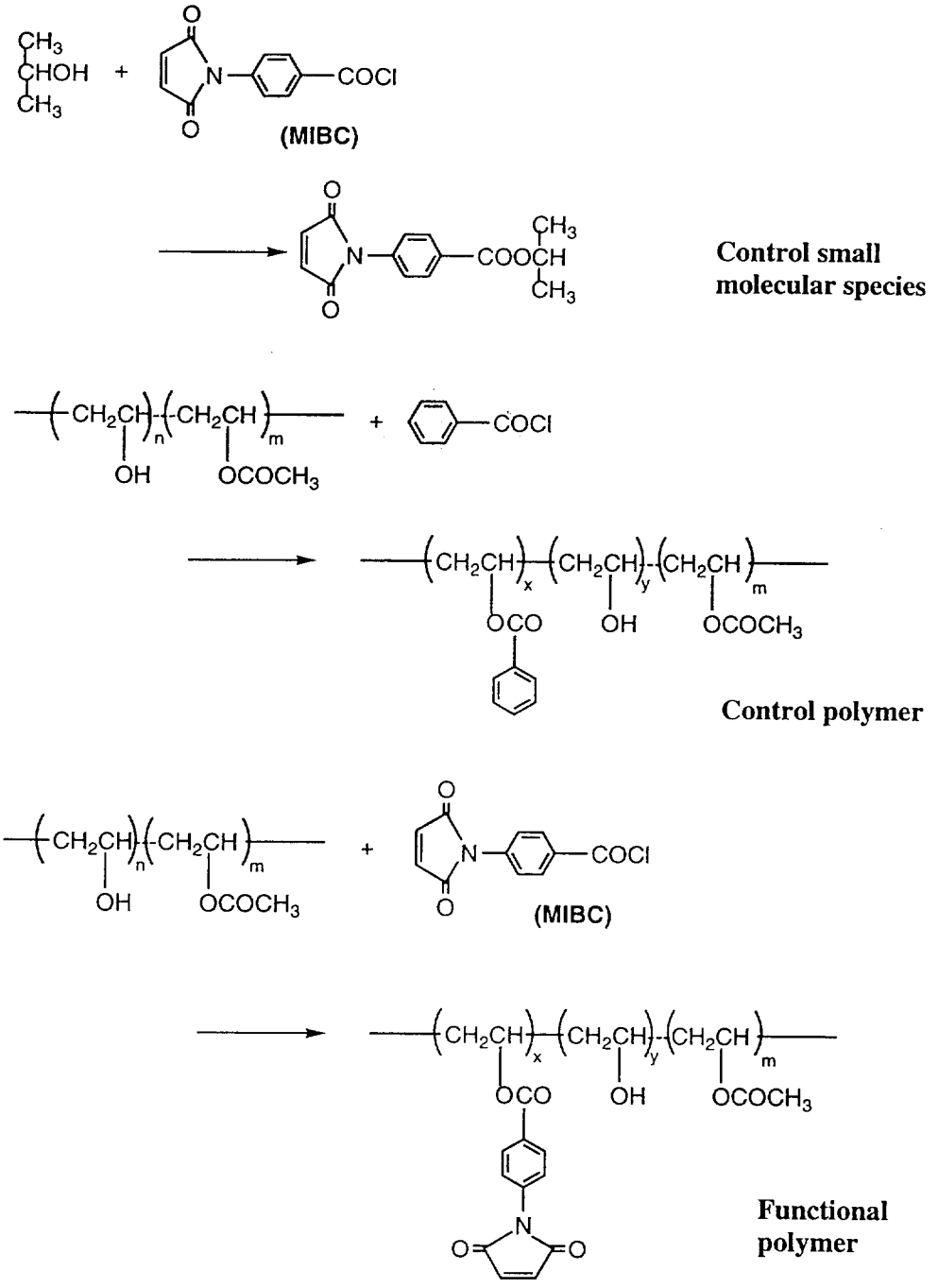

Scheme 4.1 Schematic representation of modification of partially hydrolyzed PVA and control reaction

Appendix

Pervaporation Studies Using Novel Polymer Membranes

1 Introduction

Pervaporation has been proven to be a convenient and economical technique in the case of difficult separations such as breaking azeotropes, and separation of close-boiling and heat-sensitive liquid mixtures. To establish pervaporation as a competitive separation process, various strategies have been applied to develop novel membranes and modules. In this research, a novel pervaporation membrane with maleimide derivatives covalently coupled to a glassy polymer backbone has been developed to facilitate separating styrene from styrene/ethylbenzene mixtures. Complexation of MIBC with styrene and ethylbenzene have been fully discussed in Chapter 3. The questions raised here are:

(1) Does this complexation have influence on the transport of styrene and ethylbenzene through the membranes? and,

(2) How does this complexation effect transport of the permeates?.

To answer these questions, a home-built pervaporation cell will be used to evaluate separation efficiency of these novel polymer membranes and, based on the sorption-diffusion model, a new separation mechanism related to the influence of permeant-membrane interaction on sorption, diffusion and transport of permeant will be established. Knowledge of the mechanism of transport in pervaporation will provide a guideline to the criteria of membrane selection and the application of this technique to various separations.

1.1 Sorption-diffusion model

Selective transport of a specific component in a mixture through a polymer membrane in pervaporation can be described by the sorption-diffusion model [13]. Permeability of each liquid component towards a polymer membrane is the product of solubility and diffusivity of the liquid component in the polymer membrane. Solubility is a thermodynamic parameter and gives a measurement of the amount of liquid component sorbed into the membrane under equilibrium conditions. Diffusivity is a kinetic parameter which indicates how fast a penetrant is transported through the membrane. In the sorption-diffusion model, existence of thermodynamic phase equilibria at both membrane boundary surfaces in contact with both the feed solution and the permeate solution is assumed. It is also assumed that diffusion of each component through the membrane obeys Fick's law. Permeation of the component through the membrane is represented by non-equilibrium thermodynamics. Permeant flux of the i component, J_i, is expressed by

$$J_i = \sum_j L_{ij} X_j \qquad (1)$$

where L_{ij} are phenomenological coefficients and X_j are generalized forces. When this relation is considered for mass transport in pervaporation, equation (1) becomes:

$$J_i = \sum_j D_{ij} [\frac{\partial u}{\partial x}]_j \qquad (2)$$

where D_{ij} and $[\partial u/\partial x]_j$ are thermodynamic transport coefficients and chemical potential gradients, respectively. The chemical potential gradient is the driving force in pervaporation, which can be related to an activity gradient based on the Gibbs free energy:

$$\mu_j = \mu_0 + RT ln a_j \qquad (3)$$

where μ_0 is standard chemical potential of component j, a_j is activity coefficient of component j which can be represented as the product of activity coefficient and concentration of component j, C_j, respectively. Permeant flux can be rewritten as

$$J_i = \sum_j D_{ij} \frac{\partial C_j}{\partial x} \tag{4}$$

the generalized force can also be represented in terms of friction:

$$X_i = f_i v_i = f_i \frac{J_i}{\overline{C_i}} \tag{5}$$

where f_i, v_i and $\overline{C_i}$ are the friction coefficient, linear velocity and average concentration of component i in the system respectively. In transport of liquid components in mixtures through the membrane, the generalized force of component i is the chemical potential gradient of the component. Then equation (4) becomes:

$$J_i = -\frac{\overline{C_i}}{f_i} \cdot \frac{\partial \mu_i}{\partial X} \tag{6}$$

The relationship of the diffusion coefficient of component i with the friction coefficient can be described by Einstein's equation:

$$D_i = \frac{RT}{f_i} \tag{7}$$

Combining equation (6) and (7), permeant flux is derived as:

$$J_i = -\frac{D_i \overline{C_i}}{RT} \cdot \frac{\partial \mu_i}{\partial x} \tag{8}$$

As discussed before, the chemical potential gradient of a chemical component can be related to the concentration gradient of the component according to the Gibbs free energy. Flux of component i in the membrane with thickness x can be devised as:

$$J_i = S_i D_i \frac{\Delta C_i}{\Delta x} \tag{9}$$

$$S_i = \frac{\overline{C_i}}{C_i} \tag{10}$$

$$P_i = S_i D_i \tag{11}$$

where S_i is the solubility coefficient and P_i is the permeability coefficient of component i towards the membrane.

In equation (9), permeation of each component through the membrane was treated mathematically. As discussed before, the permeability coefficient is equal to the product of solubility coefficient and diffusion coefficient. Selective permeation is controlled by sorption of penetrant into the membrane and diffusion of penetrant through the membrane.

For single component transport through membranes, permeant flux is the product of concentration and linear velocity where velocity is the product of mobility and driving force of transport.

$$J_i = v_i c_i = -c_i B_i \frac{\partial \mu_i}{\partial x} \tag{12}$$

Under ideal conditions, equation(12) can be transformed to

$$J_i = -D_i(c) \cdot \frac{\partial C_i}{\partial x} \tag{13}$$

Permeant flux is the product of the diffusion coefficient and the concentration gradient. When a pervaporation setup is used for single component transport through a membrane, permeant is removed by a vacuum or sweepgas. Pure liquid is in contact

with the membrane directly on the feed side. It is assumed that membrane interfaces are in thermodynamic equilibrium with both the permeant and feed solution. So the chemical activity and activity gradient of the liquid just inside the membrane are directly related to the interaction between the liquid and the polymer and the activity of the liquid in both feed and permeant. Therefore, permeability of single component in the membrane is strongly dependent on liquid-polymer interactions. Solubility and diffusivity become concentration dependent.

Transport of liquid mixtures through polymer membranes is not only determined by interaction of single components with the membrane, affecting its transport through the membrane, but also by mutual interactions between components and interactions of polymer with other components affecting the transport. In other word, not only does the concentration of each component effect transport of liquid mixtures, but composition of the mixture will also effect transport, and transport of the component is influenced by flow coupling and thermodynamic interactions.

For a binary liquid transport through membranes, non-equilibrium thermodynamics can be used to describe permeant flux [65]:

$$-J_1 = L_{11}\frac{\partial \mu_1}{\partial x} + L_{12}\frac{\partial \mu_2}{\partial x} \tag{14}$$

$$-J_2 = L_{21}\frac{\partial \mu_1}{\partial x} + L_{22}\frac{\partial \mu_2}{\partial x} \tag{15}$$

Permeant flux of a component consists of the flux due to its own driving force and the flux due to the coupling effect of another component in the mixture. Permeant flux is not only effected by flow coupling, but also strongly dependent on thermodynamic interactions among components and between polymer and permeates. The important concept is that thermodynamic interaction dependence of solubility and diffusivity of each component in mixtures determines preferential sorption and diffusion which, in

turn, determine selectivity of the membrane toward the component in mixtures to be separated.

1.2 Sorption

Membrane sorption depends on interactions between the membrane and the penetrants. In pervaporation, where interaction between membrane and liquid/vapor are generally strong, sorption of liquid and vapor into the membrane can no longer be described by Henry's law. Instead, it is best described by Flory-Huggins thermodynamics [66].

Solubility of a pure liquid in a polymer can be expressed as a free enthalpy of mixing ΔG_m of a binary mixture consisting of the pure liquid and the polymer:

$$\Delta G_m = RT(n_l \ln\phi_l + n_p \ln\phi_p + \chi_{lp} n_l \phi_p) \qquad (16)$$

where, ϕ_l, ϕ_p are volume fraction of the pure liquid inside of the polymer and the polymer, respectively. χ_{lp} is the liquid-polymer interaction parameter.

At sorption equilibrium:

$$ln a_l = \frac{\partial(\Delta G_m)}{\partial n_l} \cdot \frac{1}{RT} = \ln\phi_l + \phi_p\left(1 - \frac{V_l}{V_p}\right) + \chi_{lp}\phi_p^2 = 0 \qquad (17)$$

where a_l is the activity of the pure liquid, v_l and v_p are molar volumes of the pure liquid and the polymer, respectively.

According to equation (17), the amount of pure liquid sorbed into the polymer membrane, ϕ_l (volume fraction of pure liquid inside the polymer membrane), can be calculated if the interaction parameter, χ_{lp}, is known. Similarly, the interaction parameter can be calculated from this equation when the amount of the liquid sorbed into the polymer membrane can be determined experimentally. If the polymer is completely soluble in liquid, the interaction parameter χ_{lp} is less than 0.5. With decreasing affinity between polymer and liquid penetrant, the value of χ_{lp} will increase.

When polymer is only swollen in liquid, χ_{1p} is usually higher than 0.5.

In pervaporation, liquid mixtures are usually dealt with instead of pure liquid. In this case, sorption of a component in liquid mixtures is not only dependent on its own interaction with the polymer membrane, but also influenced by mutual interactions between components and interactions between other components and the polymer membrane. Preferential sorption of a specific component in mixtures, which represents sorption selectivity of membrane, as well as overall sorption into membrane must both be considered.

Similar to binary systems, free enthalpy of mixing is used to characterize permeant sorption and preferential sorption in ternary systems containing liquid component 1 and 2 in a liquid mixture and the polymer.

$$\Delta G_m = RT(n_1 \ln\phi_1 + n_2 \ln\phi_2 + n_p \ln\phi_p + \chi_{12} n_1 \phi_2 + \chi_{1p} n_1 \phi_p + \chi_{2p} n_2 \phi_p) \qquad \textbf{(18)}$$

where ϕ_1, ϕ_2 are volume fractions of liquid component 1 and 2 inside the polymer membrane, respectively. ϕ_p is the volume fraction of the polymer membrane. χ_{12}, χ_{1p}, χ_{2p} are the Flory-Huggins interaction parameters.

$$\ln a_1 = \ln\phi_1 + \phi_1\left(1 - \frac{V_1}{V_2}\right) + \phi_p\left(1 - \frac{V_1}{V_p}\right) + (\chi_{12}\phi_2 + \chi_{1p}\phi_p)(\phi_2 + \phi_p) - \chi_{2p} \cdot \frac{V_1}{V_2} \cdot \phi_2 \cdot \phi_p \qquad \textbf{(19)}$$

$$\ln a_2 = \ln\phi_2 + \phi_1\left(1 - \frac{V_2}{V_1}\right) + \phi_p\left(1 - \frac{V_2}{V_p}\right) + (\chi_{12}\phi_1 + \chi_{2p}\phi_p) \cdot (\phi_1 + \phi_p) - \chi_{1p} \cdot \frac{V_2}{V_1} \cdot \phi_1 \cdot \phi_p \qquad \textbf{(20)}$$

At sorption equilibrium, chemical potentials of individual components in the feed solution and inside the polymer membrane should be the same. Under this condition,

the relationship of

$$\ln(\frac{\phi_1}{\phi_2}) - \ln(\frac{V_1}{V_2}) = (l-1)\ln\phi_2/V_2 - \chi_{12}(\phi_2-\phi_1) - \chi_{12}(V_1-V_2) - \phi_p(\chi_{1p}-l\cdot\chi_{2p}) \quad (21)$$

can be devised, where V_1, V_2 are molar volumes of components 1 and 2 in the feed solution, respectively and l is the ratio of molar volume of components 1and 2 (V_1/V_2). From this equation, sorption selectivity is defined as

$$\alpha_{sorp} = \frac{(\phi_1/\phi_2)}{(V_1/V_2)} \quad (22)$$

It can be calculated when interaction parameters and the ratio of molar volume l and volume fraction of the polymer ϕ_p are known. It can be seen that the affinity of liquid components towards the polymer membrane and mutual interactions of components, expressed as interaction parameters, play important roles in promoting preferential sorption. High affinity of a component towards the polymer membrane always leads to preferential sorption of this component. In addition, preferential sorption of the component is influenced by affinities of other components to polymer membrane and mutual interactions of components in mixtures. In all of these discussions, the Flory-Huggins interaction parameters are assumed to be concentration independent. However, the generally influence of concentration on the interaction parameters should be considered.

1.3 Diffusion

Diffusion is defined as the statistical molecular transport across an activity gradient, which is generally expressed by Fick's Law

$$J_i = -D_i(c) \cdot \frac{dc_i}{dx} \tag{23}$$

Flux J of a component through a plane perpendicular to the direction of diffusion is proportional to the concentration gradient. The proportionality constant is called the diffusion coefficient.

In the case of a gas permeating through a polymer membrane, normal interactions between gas and polymer are small and consequently, the influence of gas on polymer structure and segmental motions can be neglected. Therefore, the diffusion coefficient can be considered as a constant. In pervaporation, the structure and segmental motions of polymer in the separation membrane is largely affected by sorption of liquid and/or vapor inside the membrane. When a polymer membrane is internally saturated with a sorbed liquid, diffusion of penetrants is more like diffusion through a liquid than a solid polymer membrane. Thus, the diffusion coefficient becomes concentration dependent. The Fujita free volume theory was developed to interpret the concentration dependence of the diffusion coefficient. In this theory, diffusion of a molecule in the polymer membrane is viewed as a series of activated jumps from location to location if there is sufficient empty space or free volume. Free volume, V_f, is defined as the volume generated by thermal expansion of initially close-packed molecules at 0°K:

$$V_f = V_T - V_0 \tag{24}$$

where V_T is the observed volume at temperature T, and V_0 is the volume of close-packed molecules at 0 K. Fractional free volume is defined as the ratio of free volume to the observed volume:

$$v_f = \frac{V_f}{V_T} \tag{25}$$

In a system where penetrant highly interacts with the polymer membrane, free volume

of the system is a function of temperature and volume fraction of the diffusing species:

$$v_f(v_p,T) = v_f(0,T) + \beta(T)\cdot v_p \quad (26)$$

where $v_f(v_p,T)$ is the functional free volume of the system containing polymer and penetrants with volume fraction, v_p, $v(0, T)$ is fractional free volume of polymer without penetrant, and $\beta(T)$ is a proportionality factor related to the volume fraction of penetrants inside the polymer.

The probability of finding a jump position with sufficient free volume is proportional to exp[-B/v(0,T)], where B expresses the local free volume needed for a given penetrant. Mobility of the given penetrant depends on the probability of finding a position with enough free volume to allow its displacement. Mobility can be related to the thermodynamic diffusion coefficient by

$$D_T = RTA_f\exp(-B/v_f) \quad (27)$$

Here, A_f is dependent on the size and shape of the penetrant molecules while B is related to the minimum local free volume necessary to allow a displacement. According to this equation, the diffusion coefficient at zero penetrant concentration is

$$D_0 = RTA_f\exp[-B/v_f(0,T)] \quad (28)$$

and the thermodynamic diffusion coefficient is

$$D_T = RTA_f\exp[-B/v_f(v_p,T)] \quad (29)$$

Combining equations (28) and (29), the diffusion coefficient is expressed as a form of Fijita's free-volume theory:

$$(\ln\frac{D_T}{D_0})^{-1} = \frac{v_f(0,T)}{B} + \frac{v_f(0,T)^2}{\beta(T)\cdot B\cdot v_p} \quad (30)$$

The concentration dependence of the diffusion coefficient is clearly shown in this equation. $[\ln(D_T/D_0)]$ has a linear relationship with v_p. As the concentration dependence of diffusion is due to interaction of penetrant with polymer, the observed diffusion coefficient is related to the thermodynamic diffusion coefficient in terms of

penetrant activity:

$$D_i = (D_T)_i \cdot (1 - v_i) \cdot \frac{\partial ln a_i}{\partial ln v_i} \qquad (31)$$

The influence of interaction between penetrant and polymer on the activity of the components is expressed by the Flory-Huggins thermodynamics as discussed above in this Chapter.

It can be seen that diffusion of liquid penetrants through polymer membranes is largely affected by interactions between penetrants and polymer. In the case of diffusing liquid mixtures through polymer membranes, preferential diffusion happens due to affinity of penetrant for polymer membrane and mutual interactions among penetrants.

2 Proposed experimental methods

2.1 Pervaporation membranes preparation.

DMAc solutions of PVA and modified PVA are prepared by dissolving preweighed quantities of dry polymer in purified DMAc with stirring at 60°C for 5 hours. Homogenous polymer membranes are prepared by casting these solutions on clean glass plates. DMAc is removed by evaporation in air at room temperature followed by vacuum drying. The membrane is subsequently peeled off the glass plate. A nonporous, transparent and dense membrane is produced by this procedure. The thickness of the membrane can be measured using a micrometer.

2.2 Pervaporation module setup

The apparatus used for measuring performance of the affinity-based pervaporation membrane is shown in Figure 5.1. Figure 5.2 presents a schematic

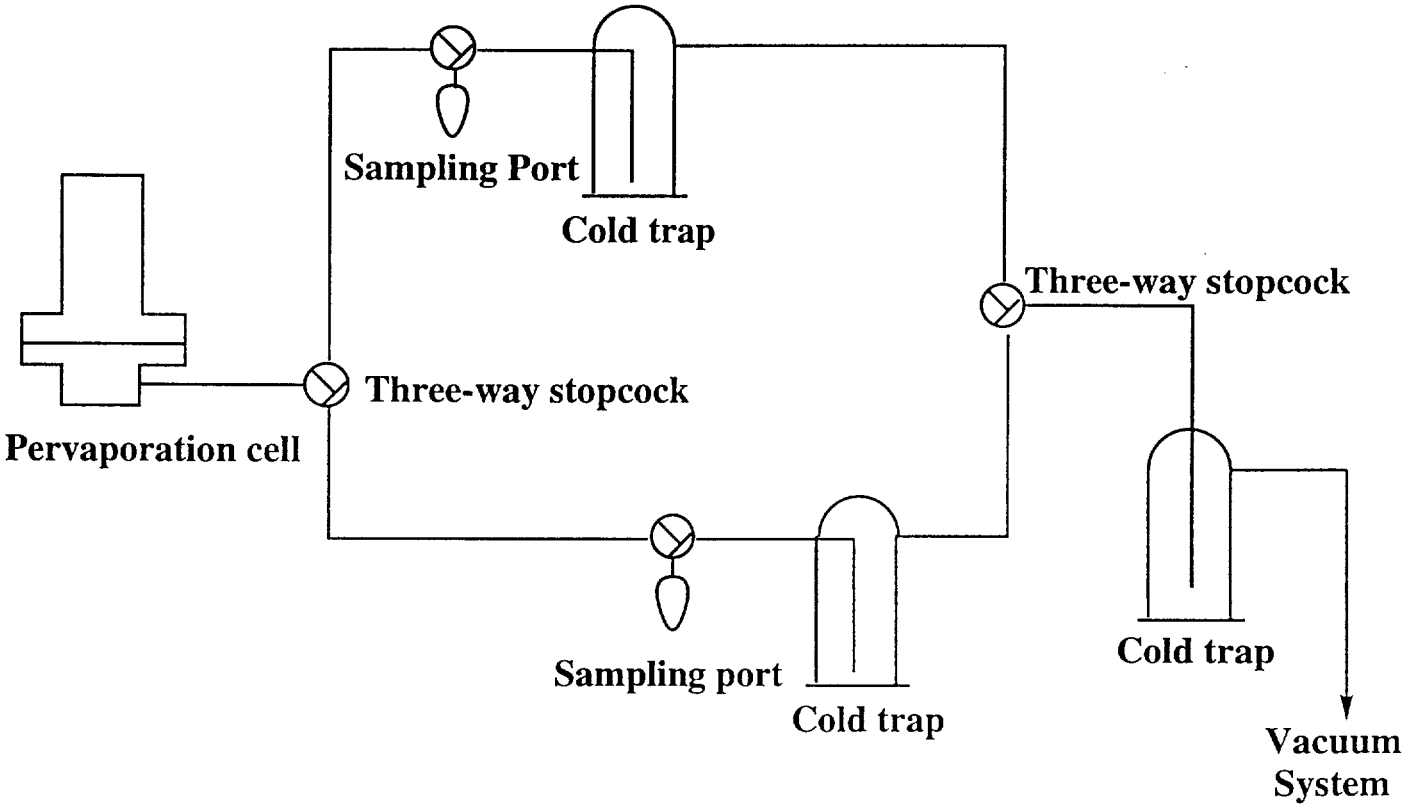

Figure 1 Experimental system for pervaporation experiments.

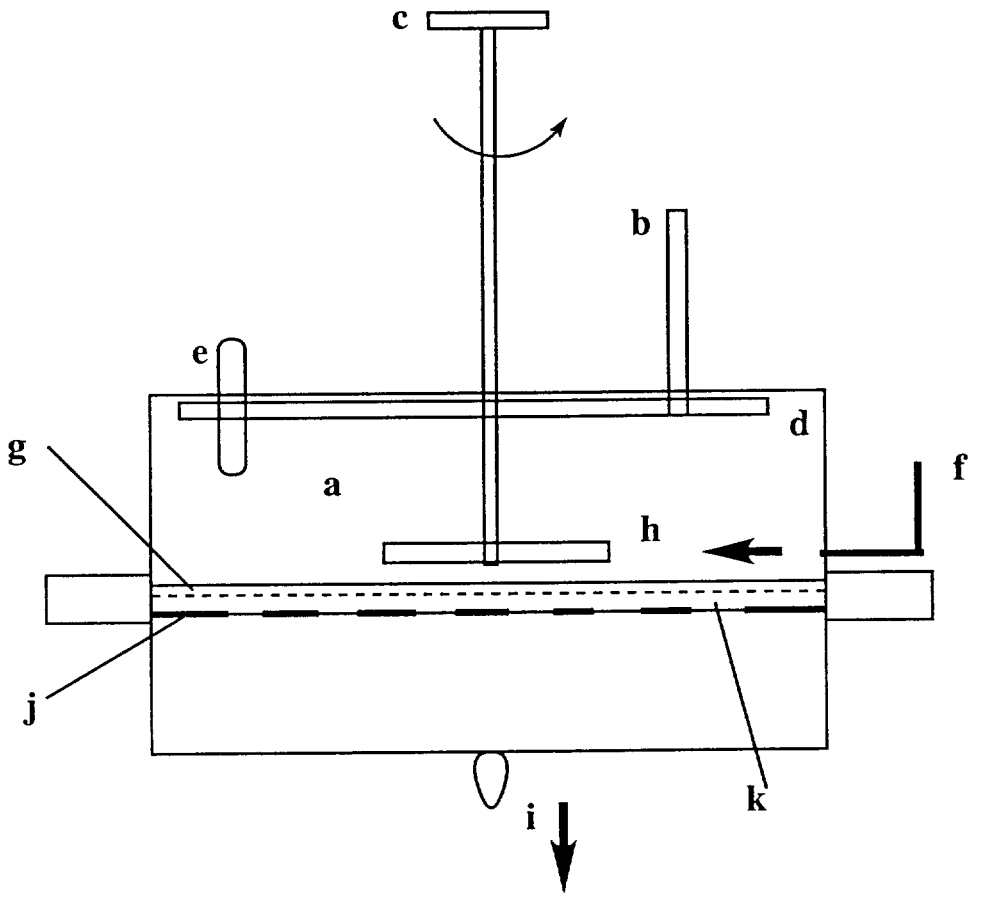

a) feed chamber
b) condenser
c) variable speed motor
d) thermostated circulation coil
e) thermowell
f) feed inlet tube
g) rubber gasket
h) stir impeller
i) vapor outlet joint
j) porous aluminum disc
k) polymer pervaporation membrane

Figure 2 Schematic representation of the pervaporation testing module.

representation of the pervaporation testing module. Fabricated membranes are supported by filter paper resting on a piece of metal mesh with 5 cm diameter. Feed solutions will be introduced to the upper glass compartment (250 ml capacity). Efficient stirring is ensured by a mechanical stirrer contained inside the upper compartment. The lower compartment is connected to cold traps and a vacuum system. Two parallel cold traps were designed in this system to remove samples while isolating the vacuum during the measurement.

2.3 Studies of pervaporation efficiency and separation mechanism

2.3.1 Solubility

Solubility of donor penetrant components in liquid mixtures in the separation membranes is measured by testing sorption and desorption of membranes in pure components and mixtures. These methods are described below.

A. Swelling ratio measurement

Pieces of membranes are immersed in pure styrene, ethylbenzene or styrene/ethylbenzene mixtures of different ratios at room temperature. The swollen membrane pieces will be removed from the liquids at regular intervals, carefully wiped with a tissue to remove adherent solvent and weighed in a closed vial. This will be continued until no further weight increases are observed. The swelling ratio indicating solubility of liquid components in the membranes is expressed as a relative weight increase of the membrane.

$$S = \frac{W_s - W_d}{W_d} \tag{32}$$

where W_d and W_s denote the weight of the dry and swollen membrane pieces, respectively.

B. Determination of solvent composition in membranes

A desorption experiment is carried out using the pervaporation apparatus. Solvent-swollen membranes are removed from the pure liquid penetrant components or liquid mixtures and carefully wiped to remove surface solvent. Solvent in the membranes will be evaporated under reduced pressure and collected in a cold trap cooled by a dry ice-acetone mixture. Composition of solvent collected from the membranes will be determined using gas chromatography. The separation factor, α_s, related to the solubility of each component towards the polymer membranes, can be calculated from the concentration ratio of solvent in the membranes and the feed solutions by:

$$\alpha_s = \frac{S_A / S_B}{F_A / F_B} \tag{33}$$

where S_A/S_B and F_A/F_B denote the concentration ratios of solvent sorbed in the membranes and in the feed solutions, respectively.

2.3.2 Pervaporation analysis

Testing of the permselectivity of the resulting membranes will be carried using the apparatus described above in Section 2.2 at room temperature. Feed solutions are introduced into the upper compartment of the pervaporation cell and vigorously stirred using a mechanical stirrer. Pressure downstream of the membrane is reduced by a vacuum pump. Permeating species are collected into cold traps. Composition and flux of permeating mixtures are determined by gas chromatography. Selective permeability of the membranes is measured with respect to permeate rate, P, and separation factor,

α. Permeate rate, P, is calculated with a correction of the flux for membrane thickness. The separation factor can be determined by measurement of the concentration ratio of the permeate and the feed solution.

2.3.3 Diffusivity

Diffusivity of each component and the coupling effects of dual-components in the membrane is be calculated from results of solubility and permeability measurements of the pure components and their respective mixtures. The diffusivity is defined as P/S

3 Discussion

Influence of interaction of the liquid components to be separated with the polymer membrane, and mutual permeant interactions on permeation and permselection has been discussed in this appendix. Permeability and selectivity of membranes derivatized with MIBC complexing groups will be tested using the experimental pervaporation measurement module. Based on the results obtained from these measurements, the influence of complexation between MIBC and donor components in permeating liquid mixtures on sorption, diffusion and permeation will be calculated. Complexation between polymer membrane functional groups and permeants in mixtures is effected by the derivatization chemistry of polymer membranes and the liquid mixture composition. Temperature and other operating conditions will also have an influence. Optimized separation efficiency will obtained by adjusting the chemistry and density of complexing groups attached to polymer chains and the pervaporation operating conditions.

References

1. Mulder, M., "Basic Principles of Membrane Technology", Kluwer Academic Publishers, The Netherlands, 1991.

2. Strathmann, H., (1991) in: Costa C.A. and Cabral J.S. (Ed.), "Chromatographic and Membrane Processes in Biotechnology", Kluwer Academic Publishers, The Netherlands, pp 153-176.

3. Bowen, R.W. in: Costa, C.A. and Cabral J. S (Ed.) "Chromatographic and Membrane Processes in Biotechnology", Kluwer Academic Publishers, The Netherlands, pp. 207-221.

4. Kimura S., *J. Chem. Eng. Japan*, 1992, 25(5), 469-480.

5. Gupta, B.D. and Mukherjee, A.K., *Ploy.-Plast. Technol. Eng.*, 1990, 29(4), 299.

6. Neel, J., in "Pervaporation Membrane Separation Processes" Huang, R. Y. M., ed., Elsevier Science Publishers B.V., Amsterdam, The Netherlands, pp 1-109, 1991.

7. Binning, R.C., Lee. R.J., Jennings, J.F., and Martin, E.C., *Ind. Eng. Chem.*, 1961, 53, 45

8. Michaels, A.S., Baddour, R.F., Bixler, H.J., and Choo, C.Y. *Ind. Eng. Chem. Proc. Deg. Develop.*, 1962, 1, 14.

9. Krewinghaus, A.B., Ph.D Thesis, Massachusetts Institute of Technollogy, Cambridge, MA, 1966.

10. Fels, M. and Huang, R.Y.M., *J. Macromol. Sci-Phys.*, 1971, bf. B5(1) 89.

11. Yoshikawa, M., Yokoi, H., Sanui, K., and Ogata, N. *J. Polym. Sci.: Polym. Chem. Ed.*, 1984, 22, 2159

12. Schrodt, V.N., Sweeny, R.F. and Rose A., *Proc. Div. Indust. Eng. Chem.* 144th Meeting, ACS, Los Angeles, 1993.

13. Lee, C.H., *J. Appl. Polym. Sci.*, 1975, 19, 83.

14. Mulder, M.H.V. in: "Prevaporation Membrane Separation Processes", Huang, R.Y.M. (Ed.), Elsevier Science Publishers B. V., Amsterdam, The Netherlands, 1991.

15. Kober, R.A., *J. Am. Chem. Soc.*, 1917, 39, 944-948.

16. Binning, R.C. and James, F.E., *Petroleum Refiner*, 1958, 37, 214-215.

17. Lee, R.J., *U.S. Patent* 2,984,623 May 16.1962

18. Binning, R. C. and Stuckey, J. M., *U.S. Patent* 2,958,657 1960

19. Binning, R.C., Jennings, J.F. and Martin, E.C., *U.S. patent* 3,035,060 1962

20. Long, R.B., *Ind. Eng. Chem.*, 1965, Fundamentals 4, 445.

21. Sweeny, R. F. and Rose, A., *Ind. Eng. Chem. Proc. Res. Develop.*, 1965, 4, 248.

22. Carter, J. W. and Jagannadhaswany, B., *Brit. Chem. Eng.*, 1964, 9, 523.

23. Warren, D., *Membr. Sep. Technol. News*, 1986, 4, 1.

24. Wenzlaff, A., Boddelker, K.W. and Hattenbach, K., *J. Membr. Sci.*, 1985, 22 333.

25. Yoshikawa, M., Yukoshi, T., Sanni, K. and Ogata N., *Polym. J.*, 1984, 14, 653.

26. Matsui, K., Ishihara, K., Tajima, R. and Nagase, Y., *Jap. patent*, 1986, 61,242,603 (Chem. Abstr. 106: 215104).

27. McCandless, F.P. and Downs, W.B., *J. Membr. Sci.*, 1987, 30, 111.

28. Nagi, E., Borlai, O., and Stelmaszek, J., *J. Membr. Sci.*, 1983, 16, 79.

29. Cabasso, I., Korngold, E. and Liu, Z., *J. Polym. Sci., Polym Lett.* 1985, 23, 577.

30. Aptel, P., Cuny, J., Jozefowicz, J., Morel, E. and Neel, J., *Eur. Polym. J.*, 1978, 14, 595.

31. Kubica, J., Kucharsky, M. and Stelmaszek, J., *Prezm. Chem.*, 1967, 6, 353.

32. Featherstone, W. and Cox, T., *Br. Chem. Eng. Proc. Techn.*, 1971, 16, 817.

33. Brun, J.P., Bulvestre, Kergreis, A. and Guillou, M., *J. Appl. Polym. Sci.*, 1974, 18, 1663.

34. Brun, J.P., Larchet, C., Bulvestre and Auclair, B., *J. Membr. Sci.* 1985, 25, 55-100.

35. Larchet, C., Brun, J.P. and Guillou, M., *J. Membr. Sci.*, 1983, 15, 81-96.

36. Cabasso, I., and Liu, Z.Z., *J. Membr. Sci.*, 1985, 24, 101-119.

37. Koops, G.H. and Smolders, C.A. in: "Pervaporation Membrane Separation Processes", Huang, R.Y.M., (Ed.), Elsevier Science Publishers, B.V. Amsterdam, The Netherlands, 1991.

38. Terada, J., Hohjoh, T., Yoshimasu, S., Ikemi, M. and Shinohara, I., *Polym.J.*, 1982, 14(5), 347-352.

39. Wilkes G.L., *J. Appl. Phys.*, 1978, 49, 5060.

40. Nagase, Y., Mori, S., Egawa, M. and Matsui, K., *Makromol. Chem.*, 1990, 191, 2413-2421.

41. Nagase, Y., Ishihara, K. and Matsui, K., *J. Polym. Sci.: Part B: Polym.Phys.*, 1990, 28, 377-386.

42. Nagase, Y., Sugimoto, K., Takamura, Y. and Matsui, K., *J. Appl. Polym. Sci.*, 1991, 43, 1227-1232

43. Yoshikawa, M., Yokoi, H., Sanui, K. and Ogata, N., *J. Polym. Sci. Polym. Lett. Ed.*, 1984, 22, 125.

44. Yoskikawa, M., Yukoshi, T., Sanui, K. and Ogata, N., *Macromolecule*, 19, 1986, 47.

45. Choy, E.M., Evans, D.F. and Cussler, E.L., *J Am. Chem. Soc.*, 1974, 96, 7058.

46. Koval, C.A., Spontarelli, T. and Noble, R. D., *Ind. Eng. Chem. Res.*, 1989, 28, 1020-1024.

47. Koval, C. A., Spontarelli, T. and Noble, R.D., *Ind. Eng. Chem. Res.*, 1989, 28, 1020.

48. Shimidzu,T., and Yoshikawa, M., in "Pervaporation Membrane Separation Processes", Huang, R. Y. M., (Ed.), Elsevier Science Publishers B.V., Amsterdam, The Netherlands, 1991.

49. Baker, R.W., Cussler, E.L., Eykamp, W., Koros, W.J., Riley, R.L. and Strathmann, H., "Membrane Separation Systems - A Research & Development Needs Assessment," 1988, DE-ACo1-88ER30133.

50. Lewis, G.N., "Valency and the structure of Atoms and Molecules", Reinhold, New York, 1923.

51. Andrews, L.J., and Keefer, R. M., *J. Am. Chem. Soc.*, 1953, 75, 3776-3779.

52. Abayasekara, D. R. and Ottenbrite, R. M., *Polym. Prepr.*, 1986, 27(1), 462.

53. Walling, Briggs, Wolfstrirn and Mayo, *J. Am. Chem. Soc.*, 1948, 70, 1537.

54. Barb, W.G., *Trans. Fara. Soc.*, 1953, 49, 143.

55. Searle, N.E., *U.S. Pat.* 2,444,536, 1948.

56. Foster, R., "Organic Charge-Transfer Complexes", Academic Press, London and New York, 1969.

57. Brackman, W., *Recl. Trav. Chim. Pays-Bas Belg,* 1949, 68, 147.

58. Benesi, H.A. and Hildebrand, J.H., *J. Am. Chem. Soc.*, 1947, 71, 2703.

59. Ketelaar, J.A.A., van de Stolpe, C., Goudsmit, A., and Dzcubas, W., *Recl. Trav. Chim. Pays-bas Belg.*, 1952, 71, 1104.

60. Hanna, M.W. and Ashbaugh, A.L., *J. Phys. Chem.*, 1964, 68, 811.

61. Berkelay, P.J., Jr. and Hanna, M.W., *J. Phys. Chem.*, 1963, 67, 846.

62. Abayasekara, D. and Ottenbrite, R.M.. *Polym. Prepr.*, 1985, 26(2), 285.

63. Foster, R. and Horman, I., *J. Chem. Soc.*, 1966, (B), 171.

64. Kuroda,H., Amano, T., Ikemoto I. and Akamatu, H., *J. Am. Chem. Soc.*, 1967, 89, 6056.

65. Mulder, M.H.V., in "Pervaporation Membrane Separation Process", Huang, R.Y.M., (Ed.) Elsevier Science Publishers B.V., Amsterdam, The Netherlands, p225, 1991.

66. Flory, P., "Principles of Polymer Chemistry", Cornell University Press, 1953.

Biographical Sketch

The author graduated from Peking University in the fall of 1989 with a B.S. degree in Chemistry, and then worked at the Chinese Science Academy as a Research Associate for two years. In 1991 she enrolled at the Oregon Graduate Institute for her M.S. degree. She has subsequently been employed by a small pharmaceutical company in the San Francisco Bay area.